

**WL-TR-97-4115**

**PLASMA-SPRAYED COATINGS AS  
SURFACE TREATMENTS OF  
ALUMINUM AND TITANIUM  
ADHERENDS**



**G. D. Davis and B. S. Wenner  
DACCO SCI, Inc.  
Columbus MD**

**P. L. Whisnant  
National Semiconductor  
Annapolis Junction MD**

**G. B. Groff  
ISPA  
Baltimore MD**

**R. Zatorski  
Zatorski Coatings Company  
East Hampton CT**

**J. D. Venables  
Venables and Associates  
Baltimore MD**

**NOVEMBER 1996**

**FINAL REPORT FOR THE PERIOD 28 May 93 - 30 Nov 96**

**Approved for public release; distribution unlimited**

**MATERIALS DIRECTORATE  
WRIGHT LABORATORY  
AIR FORCE MATERIEL COMMAND  
WRIGHT-PATTERSON AIR FORCE BASE, OH 45433-7734**

**DTIC QUALITY INSPECTED 4**

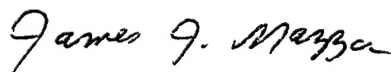
**19990713 005**

## NOTICE

USING GOVERNMENT DRAWINGS, SPECIFICATIONS, OR OTHER DATA INCLUDED IN THIS DOCUMENT FOR ANY PURPOSE OTHER THAN GOVERNMENT PROCUREMENT DOES NOT IN ANY WAY OBLIGATE THE US GOVERNMENT. THE FACT THAT THE GOVERNMENT FORMULATED OR SUPPLIED THE DRAWINGS, SPECIFICATIONS, OR OTHER DATA DOES NOT LICENSE THE HOLDER OR ANY OTHER PERSON OR CORPORATION; OR CONVEY ANY RIGHTS OR PERMISSION TO MANUFACTURE, USE, OR SELL ANY PATENTED INVENTION THAT MAY RELATE TO THEM.

THIS REPORT IS RELEASABLE TO THE NATIONAL TECHNICAL INFORMATION SERVICE (NTIS). AT NTIS, IT WILL BE AVAILABLE TO THE GENERAL PUBLIC, INCLUDING FOREIGN NATIONS.

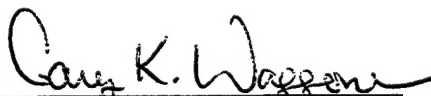
THIS TECHNICAL REPORT HAS BEEN REVIEWED AND IS APPROVED FOR PUBLICATION.



JAMES J. MAZZA  
Project Engineer  
Materials Integrity Branch



MICHAEL F. HITCHCOCK  
Chief  
Materials Integrity Branch



GARY K. WAGGONER  
Chief  
Systems Support Division

Do not return copies of this report unless contractual obligations or notice on a specific document requires its return.

REPORT DOCUMENTATION PAGE			Form Approved OMB No. 0704-0188	
Public reporting burden for this collection of information is estimated to average 1 hour per response, including the time for reviewing instructions, searching existing data sources, gathering and maintaining the data needed, and completing and reviewing the collection of information. Send comments regarding this burden estimate or any other aspect of this collection of information, including suggestions for reducing this burden, to Washington Headquarters Services, Directorate for Information Operations and Reports, 1215 Jefferson Davis Highway, Suite 1204, Arlington, VA 22202-4302, and to the Office of Management and Budget, Paperwork Reduction Project (0704-0188), Washington, DC 20503.				
1. AGENCY USE ONLY (Leave blank)	2. REPORT DATE November 1996	3. REPORT TYPE AND DATES COVERED Final 12 May 93 - 30 Nov 96		
4. TITLE AND SUBTITLE Plasma-Sprayed Coatings as Surface Treatments of Aluminum and Titanium Adherends		5. FUNDING NUMBERS C: F33615-93-C-5324 PE: 6210F/63716D PR: 2418 TA: 04 WU: FQ		
6. AUTHOR(S) G.D. Davis, B.S. Wenner, P.L. Whisnant, G.B. Groff, R. Zatoarski, and J.D. Venables				
7. PERFORMING ORGANIZATION NAME(S) AND ADDRESS(ES) DACCO, SCI, INC., Columbia MD National Semiconductor, Annapolis Junction MD ISPA, Baltimore MD Zatorski Coatings Company, East Hampton CT Venables and Associates, Baltimore MD		8. PERFORMING ORGANIZATION REPORT NUMBER		
9. SPONSORING/MONITORING AGENCY NAME(S) AND ADDRESS(ES) Materials Directorate Wright Laboratory Air Force Materiel Command Wright-Patterson AFB OH 45433-7734 POC: J. Mazza, AFRL/MLSE, 937-255-7778		10. SPONSORING/MONITORING AGENCY REPORT NUMBER  WL-TR-97-4115		
11. SUPPLEMENTARY NOTES				
12a. DISTRIBUTION AVAILABILITY STATEMENT  APPROVED FOR PUBLIC RELEASE; DISTRIBUTION UNLIMITED		12b. DISTRIBUTION CODE		
13. ABSTRACT (Maximum 200 words) Thermal sprayed coatings were evaluated as environmentally benign pretreatments for aluminum and titanium adherends. The thermal spray process allows a wide variety of coatings to be deposited onto different substrates and, hence, the coatings can be engineered for different applications. Because there are no liquid or vapor wastes for disposal, the process has several environmental advantages to conventional treatments that use strong chemicals. Scanning electron microscopy showed that the best performing treatments exhibit an irregular, rough surface over wide dimensional scales. This roughness provides excellent opportunity for mechanical interlocking or physical bonding and allows a complex interphase to be formed as the adhesive penetrates into the coating. Wedge tests prepared using the best thermal spray coatings (titanium and, in some cases, an aluminum-polyester blend) on aluminum adherends performed better under humid conditions than those prepared by the Forest Products Laboratory (FPL) process and similar to those prepared by the phosphoric acid anodized (PA) process for some adhesives. Bonds prepared using plasma sprayed titanium coatings on titanium perform equivalently to the best chemical treatments with failure within the adhesive for some adhesives.				
14. SUBJECT TERMS adhesion, surface treatment, aluminum, titanium, adhesive bonding, plasma spray, durability			15. NUMBER OF PAGES 83	
			16. PRICE CODE	
17. SECURITY CLASSIFICATION OF REPORT UNCLASSIFIED	18. SECURITY CLASSIFICATION OF THIS PAGE UNCLASSIFIED	19. SECURITY CLASSIFICATION OF ABSTRACT UNCLASSIFIED	20. LIMITATION OF ABSTRACT SAR	

## Table of Contents

<i>List of Figures</i>	<i>v</i>
<i>Foreward</i>	<i>x</i>
<i>Preface</i>	<i>ix</i>
<b>1. Introduction</b>	<b>1</b>
<b>2. Experimental</b>	<b>4</b>
<b>2.1 Materials</b>	<b>4</b>
<b>2.2 Adherend Treatments</b>	<b>5</b>
<b>2.3 Adhesion Tests</b>	<b>6</b>
<b>2.4 Characterization</b>	<b>6</b>
<b>2.5 Electrochemical Tests</b>	<b>7</b>
<b>3. Plasma Spray Treatment Evaluations</b>	<b>9</b>
<b>3.1 Aluminum Adherends</b>	<b>9</b>
3.1.1 Aluminum/Polyester and Aluminum/PEEK	9
3.1.2 Titanium and Other Metal Coatings	27
3.1.3 Alumina	35
<b>3.2 Titanium Adherends</b>	<b>40</b>
<b>4. Electrochemical Studies</b>	<b>49</b>
<b>4.1 Hydration as a Bond Failure Mechanism</b>	<b>49</b>

<b>4.2 EIS as a Bond Monitor</b>	<b>57</b>
<b>5. <i>Summary and Conclusions</i></b>	<b>63</b>
<b>6. <i>References</i></b>	<b>67</b>
<b>7. <i>List of Publications</i></b>	<b>69</b>
<b>8. <i>List of Presentations</i></b>	<b>71</b>

## List of Figures

<i>Figure 1. Tensile button pull strengths for conventional treatments and plasma spray treatments.</i>	10
<i>Figure 2. Wedge test results for FPL, PAA, grit blast, and plasma sprayed 60AlSi/40polyester treatments for Cytac FM-300M epoxy adhesive.</i>	12
<i>Figure 3. Wedge tests results for 60AlSi/40polyester plasma spray coating and FPL and PAA controls for Cytac FM-73, FM-123, and FM-300M and 3M AF-163.</i>	14
<i>Figure 4. Comparison of initial and final crack lengths of 60(Al-Si)/40polyester plasma spray treatment and control treatments for FM-123 and FM-300M adhesives.</i>	15
<i>Figure 5. Surface behavior diagram showing the locus of dry crack propagation of 60AlSi/40polyester wedge test specimens.</i>	17
<i>Figure 6. Wedge test performance of Al/polyester and pure polyester treatments using FM-300M adhesive.</i>	18
<i>Figure 7. Average initial and final crack lengths as a function of AlSi concentration for wedge tests using plasma sprayed AlSi/polyester coatings and the four adhesives.</i>	19
<i>Figure 8. SEM micrographs of 60AlSi/40polyester and 100Al plasma sprayed surfaces prior to bonding.</i>	20
<i>Figure 9. SEM micrograph of 60AlSi/40polyester surface prior to bonding.</i>	20
<i>Figure 10. Initial and final crack lengths for wedge test specimens with 60AlSi/40polyester coatings as a function of coating thickness.</i>	22
<i>Figure 11. SBD showing dry failure surfaces of wedge tests for several AlSi/polyester coating compositions.</i>	22

<i>Figure 12. Wedge test results comparing original and electrostatic reduced mixing of 60%AlSi/40%polyester.</i>	24
<i>Figure 13. Wedge tests results for plasma sprayed PEEK and 60Al/40PEEK coatings and FPL and PAA controls.</i>	25
<i>Figure 14. Initial and final crack length results as a function of Al concentration for wedge test specimens with plasma sprayed Al/PEEK coatings.</i>	26
<i>Figure 15. Wedge test results for Ti-6Al-4V coatings on 2024 Al compared to PAA and FPL controls.</i>	28
<i>Figure 16. Wedge tests results for subsequent Ti-6Al-4V coatings on Al. The adhesive was Cytec FM-73.</i>	30
<i>Figure 17. SEM micrographs of Ti-6Al-4V coated aluminum.</i>	32
<i>Figure 18. Wedge tests results showing the effect of Cytec BR-127 primer.</i>	33
<i>Figure 19. Wedge tests results for plasma sprayed and two-wire arc sprayed Ni/Al coatings compared to the chemical controls.</i>	34
<i>Figure 20. SEM micrograph of plasma sprayed NiAl coating (PS#2).</i>	35
<i>Figure 21. Early wedge test results for alumina and alumina/aluminum plasma sprayed coatings.</i>	36
<i>Figure 22. Wedge test results for plasma sprayed alumina specimens compared to chemical controls.</i>	38
<i>Figure 23. SEM micrograph of 2-mil Al<sub>2</sub>O<sub>3</sub> coating showing little opportunity for mechanical interlocking.</i>	38
<i>Figure 24. Wedge test performance of titanium treatments using Cytec FM-300M.</i>	41

<i>Figure 25. Subsequent wedge test involving plasma sprayed Ti-6Al-4V coatings on Ti-6Al-4V adherends.</i>	43
<i>Figure 26. Wedge test results showing plasma sprayed Ti-6Al-4V coatings on Ti-6Al-4V adherends.</i>	44
<i>Figure 27. Wedge test results showing plasma sprayed Ti-6Al-4V coatings on Ti-6Al-4V adherends.</i>	45
<i>Figure 28. Wedge test results showing plasma sprayed Ti-6Al-4V coatings on Ti-6Al-4V adherends.</i>	47
<i>Figure 29. Wedge test results for titanium chemical control treatments for both Cytec FM-73 and FM-300M.</i>	48
<i>Figure 30. Bode representation of EIS data -- impedance magnitude versus frequency -- for open-faced aluminum bond immersed in hot water.</i>	50
<i>Figure 31. Bode representation of EIS data -- phase angle versus frequency -- for open-faced aluminum bond immersed in hot water.</i>	50
<i>Figure 32. Near dc impedance (measured at 100 Hz) for the open-faced aluminum bond as a function of immersion time.</i>	51
<i>Figure 33. Breakpoint frequency for the open-faced aluminum bond as a function of immersion time.</i>	51
<i>Figure 34. Near dc impedance as a function of time for aluminum specimens immersed in 75°C water.</i>	53
<i>Figure 35. Near-dc impedance of wedge test specimens as a function of time.</i>	58
<i>Figure 36. Near-dc impedance of wedge test specimens as a function of crack length.</i>	58

*Figure 37. Magnitude of the impedance at 3.3 Hz as a function of time since crack initiation for the wedge test specimen.* \_\_\_\_\_ 61

*Figure 38. Near-dc impedance of wedge test specimens (FPL, FM-123) as a function of crack length.* \_\_\_\_\_ 62

## **Preface**

This program began at Martin Marietta Laboratories in Baltimore, MD. Midway into the second phase of the program, Lockheed Martin closed the Laboratories. The Principal Investigator joined DACCO SCI, INC., a small company in Columbia, MD. With the approval of the Air Force, the contract was novated from Lockheed Martin to DACCO SCI. Under a separate agreement, instrumentation and laboratory equipment needed for this program was sold to DACCO SCI. DACCO SCI then entered into subcontracting agreements for plasma spray services with ISPA of Baltimore, MD and Zatorski Coatings Company of East Hampton, CT. The plasma sprayer and plasma spray equipment at ISPA were originally at Martin Marietta Laboratories and performed all the spraying in the first part of the program. Zatorski Coating Company had performed similar work on another Wright Laboratories-sponsored project.

This program was funded by Wright Laboratory, Materials Directorate and the Strategic Energy Research and Development Program (SERDP). The contract monitor was Jim Mazza.

The authors would like to acknowledge valuable discussions with H.M. Clearfield, J.A. Dillard, D.C. Nagle, and T.J. Reinhart. Many of the micrographs, for which the authors are grateful, were taken by R. Turner of the University of Cincinnati. They are also highly appreciative of Cytec and 3M for the donation of their adhesives.

## Foreword

Plasma-sprayed coatings have been evaluated as surface treatments for aluminum and titanium adherends. For aluminum adherends, two coating compositions hold promise: 1) a 60% (aluminum-12%silicon alloy) and 40% polyester composite and 2) a Ti-6Al-4V coating. For FM-300M epoxy adhesive, the aluminum/polyester coating gives wedge test crack growth equivalent to phosphoric acid anodization (PAA). For stronger adhesives such as FM-123 or FM-73, its performance is controlled by the strength of the polyester and final crack lengths are between those of the optimized Forest Products Laboratory (FPL) etch and PAA. The titanium coating stabilizes the aluminum surface against hydration/corrosion and can give wedge test crack growth equivalent to that of PAA for FM-73. Both coatings give optimum performance with a thickness of 50  $\mu\text{m}$  (2 mils). For titanium adherends, a 50- $\mu\text{m}$  plasma-sprayed Ti-6Al-4V coating can provide identical performance to the best chemical treatment (chromic acid anodization, CAA) with crack propagation entirely within the FM-300M adhesive during wedge tests. For FM-73 adhesive, a primer appears to be needed for plasma sprayed Ti-6Al-4V coatings to approach the performance of the CAA treatment. Similar performance is observed for the Turco 5578 treatment and is attributed to the larger scale roughness of these surfaces compared to the CAA surface. Titanium coatings on both aluminum and titanium adherends showed variability in performance resulting from uncontrolled raw material variations or processing conditions. Such variability would need to be controlled prior to production use. These plasma-sprayed coatings avoid the disposal and envi-

ronmental costs of conventional chemical treatments using chromates and strong acids or bases. They also are well suited to repair or refurbish existing components.

In a separate aspect of the program, electrochemical impedance spectroscopy (EIS) measurements were used to study the stability of an aluminum bond immersed in water and to evaluate use of this technique for nondestructive evaluation of an adhesive joint. An open-faced aluminum adhesive joint immersed in hot water for six months exhibited hydration under the adhesive that caused the hydration product to erupt through the adhesive film. If a second adherend had been bonded as in a conventional joint, the stresses induced by the added volume of hydration product would have induced bond failure. This experiment is the first to definitely demonstrate hydration under an adhesive with no nearby crack and validates the theory that hydration can cause crack propagation in moist environments. EIS measurements of this sample during immersion showed that the hydration can be detected electrochemically. Subsequent experiments involving wedge tests show that EIS is a very sensitive probe of the presence of moisture in a bondline. Because moisture is the primary cause of environmentally induced degradation of aluminum adhesive joints, this technique has the potential to detect bond degradation nondestructively before delamination.

## 1. Introduction

Conventional surface treatments of aluminum and titanium adherends [such as the Forest Products Laboratory (FPL) etch, phosphoric acid anodization (PAA), chromic acid anodization (CAA), Turco 5578 etch, and Pasa-Jell 107 etch] contain chromates and involve strong acids and/or bases in one or more of the processing steps and usually in the primer. Chromates are known carcinogens and toxins. They are strictly regulated by the Environmental Protection Agency (EPA) and the Occupational Safety and Health Administration (OSHA). Disposal of chromates and strong acids/bases is expensive, and costs are expected to rise. Expensive disposal and handling problems of chromates and other toxic materials call for new surface treatments.

Nonchemical surface treatments can eliminate or reduce much of the liquid and vapor waste ultimately released into the hydrosphere or the atmosphere. They have other potential advantages of being more suited for repair/refurbishment and less sensitive to metallurgical differences from alloy to alloy.

Plasma spraying is one such treatment that has been shown to provide excellent high-temperature bond performance with titanium (unlike conventional oxidization treatments).<sup>1</sup> Success has also been reported using alumina and other coatings on aluminum<sup>2-4</sup> as well as passive metal coatings on steel.<sup>5</sup> Plasma spraying has the important advantage of versatility. A wide range of coatings (metals, ceramics, and polymers) can be deposited onto an equally wide range of substrates and the coating properties can be optimized for a given application, independent of the substrate. Because of this versatility, plasma-sprayed coatings have been used for wear resistance, thermal barri-

ers, EMI/RF shielding, corrosion resistance, slip/slide resistance, and biocompatibility in addition to adhesion. If desired, the composition and, hence, the properties of a coating can be graded from the substrate to the surface.

In this work, we have investigated the use of alumina, aluminum, titanium, nickel-aluminum, polyester, polyetheretherketone (PEEK) and mixtures of these materials as coatings on aluminum adherends. Titanium was also evaluated as a coating on titanium adherends. Each of these materials is commonly plasma-sprayed. Alumina was chosen to provide hydration and corrosion resistance to the substrate. Corundum ( $\alpha$ -alumina) is very stable and does not hydrate (unlike the amorphous aluminum oxides chemically or electrochemically grown at the moderate temperatures and voltages used in conventional processes). Preliminary results showed that plasma-sprayed alumina coatings would protect the substrate from hydration during immersion in boiling water for 3 hours. Aluminum, titanium, and nickel-aluminum were expected to be tougher than alumina and analogous to the titanium coatings previously developed for titanium.<sup>1</sup> The polymers were expected also to be tougher and to possibly act as a primer to the metal. Mixtures were selected to combine properties of the two constituents.

The adhesion results obtained using the plasma-sprayed coatings were compared with those using conventional chemical and nonchemical treatments. We examined the effect of pre-spraying surface treatment, coating thickness, spray angle, coating composition, powder mixing procedures, and adhesive on bond performance, mostly durability as determined by the wedge test.

A second aspect of the program was to investigate the use of electrochemical impedance spectroscopy (EIS) as a means to detect bond failure without having to perform

destructive mechanical tests. In particular, the goal was to detect a bond failure before the joint weakens sufficiently that separation, which can be detected by a number of nondestructive evaluation (NDE) techniques, occurs. EIS has been used to detect deterioration and delamination of organic coatings, such as paints, on steel and other substrates,<sup>6-10</sup> but not on structural adhesive joints. Previously, we were able to correlate the near dc-impedance of an EIS measurement with the tensile button strength of a painted steel substrate.<sup>11-13</sup> A linear relationship between the tensile strength and the fraction of interfacial failure suggested that the decrease in strength could be attributed to interfacial delamination and that any changes in the coating properties had a much smaller effect.

Despite the use of EIS to detect corrosion and delamination of protective coatings, little work has focused on adhesively bonded structures. The effects of several differences between painted steel and adhesively bonded aluminum on EIS measurements have not been known. In particular, the aluminum surface is generally treated to provide physical bonding that is independent of secondary chemical bonding. These secondary bonds provide the interfacial strength for painted steel, but are disrupted once moisture diffuses to the interface. Furthermore, steel readily corrodes in the presence of moisture while aluminum is much more stable and hydrates over a longer time period. The initial goal of this task was to determine if hydration under an adhesive was detectable with EIS. We then evaluated the feasibility of EIS detecting degradation in a bonded joint.

## 2. Experimental

### 2.1 Materials

Substrates were 2024-T3 or 7075-T6 aluminum or Ti-6Al-4V titanium. Unless otherwise noted, the panels were grit-blasted shortly before plasma spraying. The coatings deposited are given in Table 1. Except for the 60(Al-Si)/40polyester, which was obtained from Metco as a mix, all blends were mixed in the laboratory before spraying. The Al-Si particles are an 88%Al-12%Si alloy. To avoid unnecessarily complicating the process, no attempt was made to vary the coating composition as a function of depth.

*Table 1. Coating Compositions*

<i>Commercial Materials</i>	<i>Laboratory Mixes</i>
Al <sub>2</sub> O <sub>3</sub>	25Al/75Al <sub>2</sub> O <sub>3</sub>
Al	75PEEK/25Al
Polyester	60Al/40PEEK
PEEK	80AlSi/20Polyester
60AlSi/40Polyester	70Al/30Polyester
Ti-6Al-4V	60Al/40Polyester
Ni-Al	25Al/75Polyester

Cytec FM-123, FM-300M, FM-73, and FM-73M epoxy adhesives were used for wedge tests of aluminum. (No difference was noted between the FM-73 supported by a scrim and by a mat.) Limited experiments were performed using 3M AF-163-2. Titanium wedge tests were performed using FM-300M and FM-73(M). Tensile button pulls were

bonded with 3M 1838 room-temperature-curing epoxy. Although reasonable care was taken to bond the specimens shortly after plasma spray, it was not always possible. No difference in bond performance was noted between specimens bonded within 1 to 2 days and specimens bonded after several weeks of ambient laboratory exposure. Other studies have suggested that other plasma sprayed surfaces can be stored indefinitely in plastic bags prior to bonding. In the case of chemical controls, bonding occurred within 24 hours.

## **2.2    *Adherend Treatments***

The panels were degreased and grit-blasted either with a mixture of alumina, fused silica, silicon carbide, and crystalline silica, or with pure alumina (80 grit size). Grit blasting was performed at near-normal incidence at a pressure of 1.5 kPa. The specimens were plasma sprayed within 4 hours of grit blasting.

Plasma spraying was achieved using a Metco 7MB or 3MB plasma gun with a 7MC control console, a 40-kW rectifier, and dual 4MP or 3MP powder feeders. The gun was mounted on a robot articulated-arm for controlled, reproducible coatings. The coatings were formed with several passes of the spray to build up the desired thickness. The angle between the spray axis and the surface plane was either 45° or near 90°. To remove any moisture, the substrate was heated to ~100°C by the plasma torch by rastering the gun over the specimen prior to injecting powder into the gun. During plasma spraying, the specimens were air-cooled from the back and sides except for some of the PEEK coatings, which performed better without cooling.

Both chemical and mechanical control treatments were performed for comparison. For aluminum adherends, the chemical treatments included optimized FPL and PAA as conventional aerospace processes and P2, the chromate-free ferric sulfate/sulfuric acid etch. For titanium adherends, the surfaces were prepared with CAA, Turco 5578 etch and Pasa-Jell 107 etch. Both materials were also prepared with the same grit blast used prior to plasma spraying as a nonchemical control. The aluminum was also treated with a less controlled silica grit blast representing a more typical process.

### **2.3    *Adhesion Tests***

Initial bond strengths were measured by tensile button pulls using a pneumatic adhesion tensile testing instrument (PATTI). Aluminum stubs were given an FPL treatment prior to bonding with the room temperature adhesive.

The most discriminating test for the different surface treatments was the wedge test (ASTM D3762). One-eighth-inch (3-mm) wedges and adherends were used for both aluminum and titanium. Specimens were exposed to >95% relative humidity at 65°C for approximately 8 days. Initial crack lengths provided a measure of initial bond strength while final crack length provided a measure of durability. The locus of failure indicates the weakest component of the bondline (coating/metal interface, coating, coating/adhesive interface, or adhesive).

### **2.4    *Characterization***

Selected specimens, both as-sprayed and matching failed surfaces, were characterized with optical microscopy, scanning electron microscopy (SEM), and x-ray photoelectron

spectroscopy (XPS). The SEM micrographs were obtained on either a JEOL JSM T220-A SEM or a JEOL 100CX STEM using secondary electrons for imaging. Specimens were coated with a thin Pt or Au film for charge neutralization. XPS measurements were obtained using a Surface Science Instruments Model SSX 100-03 spectrometer with a monochromatized Al K $\alpha$  x-ray source and a hemispherical electron energy analyzer with multichannel detection. The x-ray source was focused to a spot size of 600  $\mu$ m and the surface charge was neutralized with low-energy electrons. Binding energies were normalized to that of adventitious hydrocarbon at 284.8 eV.

## **2.5 Electrochemical Tests**

To evaluate the EIS procedure, an open-faced adhesive joint was prepared by curing FM-123 adhesive to an FPL-etched aluminum disk. A Teflon release film was used on the other side of the adhesive to prevent bonding to the press. This specimen was then mounted in a Teflon fixture that isolated the edges and back from the electrolyte. The mounted specimen was immersed in a solution of 0.05 M Na<sub>2</sub>SO<sub>4</sub> to provide sufficient conductivity for testing. Initially the solution was at room temperature, but after 1 day, the temperature was increased to 58°C to speed any reactions. EIS measurements were made using a PAR Model 273 potentiostat. The data were analyzed using the Bode plots of magnitude of the impedance versus frequency and phase angle versus frequency. From time to time, the mounted specimen was removed from the solution and examined visually. It was not removed from the fixture until the end of the experiment. At that point, XPS was used to examine the surface chemistry of various points on the specimen.

Subsequent tests were performed on FPL, PAA, and polished Al with FM-123 and FM-300 adhesive. The specimens were mounted in epoxy mounting compound. They were immersed in 75°C water in a humidity chamber. From time-to-time, they were removed from the bath and mounted on a flat cell at room-temperature. After allowing the temperature to equilibrate for 30 minutes, EIS measurements were taken.

Additional EIS measurements were taken on wedge test specimens using the two adherends as the two electrodes and a ceramic wedge to electrically isolate the two adherends. Two experiments were performed – one in which the EIS measurements were made on specimens while they were out of the humidity chamber during the period that crack lengths were measured and one in which the EIS measurements were made while the specimens were in the humidity chamber before they were removed for crack length measurements.

### **3. Plasma Spray Treatment Evaluations**

#### **3.1 *Aluminum Adherends***

##### **3.1.1 *Aluminum/Polyester and Aluminum/PEEK***

The majority of the effort on the program has involved plasma sprayed Al/polyester coatings. They showed the greatest initial promise both with initial bond strength and durability.

Early in the program, initial bond strengths were determined by tensile button pulls such as those given in Figure 1 for the control treatments and several plasma spray treatments. The best plasma-sprayed specimens exhibited pull strengths equal to or greater than the chemical controls. The locus of failure of these controls was entirely within the epoxy adhesive. The same was predominately true for the plasma-sprayed specimens as well, although there were smaller areas that failed within the coating in some cases. The similarity of the pull strengths despite the mixed mode of failure suggests that the cohesive strengths of the coatings and adhesive are similar. In contrast to the chemical controls, the "optimized" grit-blasted specimen exhibited mixed mode failure, partially in the adhesive and partially between the adhesive and the substrate, and this interfacial failure is reflected in the lower strength values.

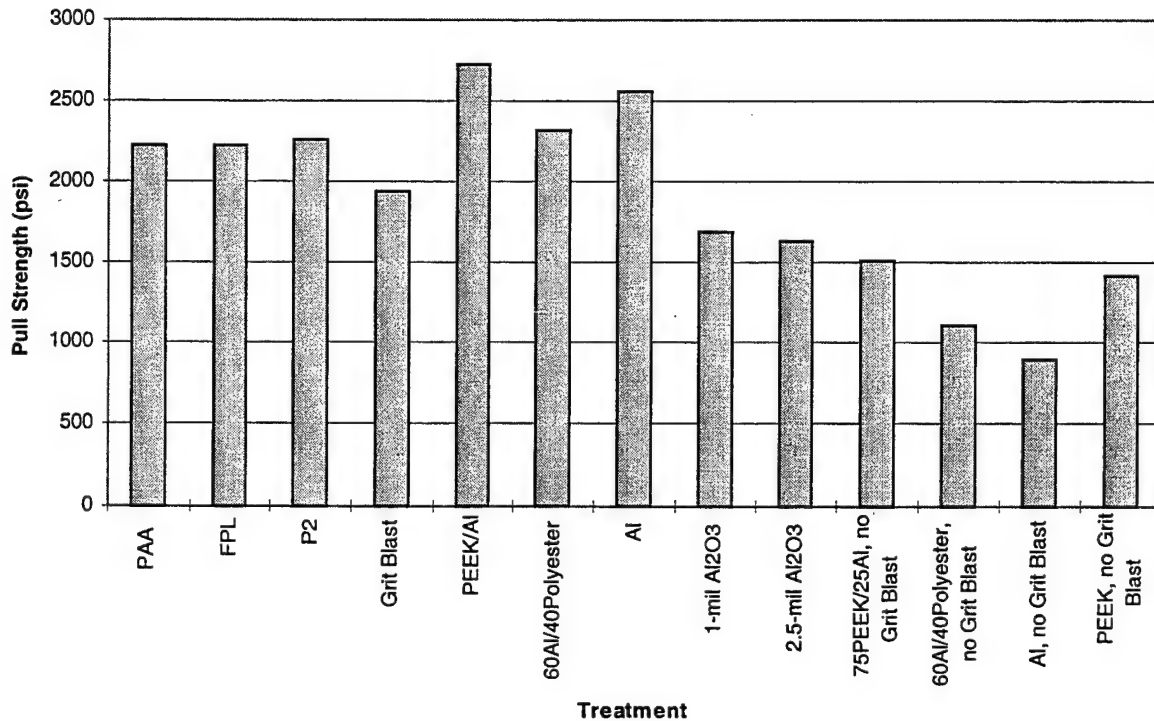


*Figure 1. Tensile button pull strengths for conventional treatments and plasma spray treatments. These and all other specimens unless otherwise indicated were prepared by the first plasma sprayer (PS#1).*

Still lower pull strengths were obtained for the alumina coatings and the coatings deposited on substrates that were not grit blasted. The alumina specimens failed within the coating itself indicating poor toughness and/or cohesive strength of the alumina. The failure mode for the coatings deposited on non-grit-blasted panels was between the coating and the substrate reflecting the need for a pretreatment, such as grit blasting, before spraying.

Although the button pull experiments gave a quantitative tensile strength value, the test was insensitive to coating performance, especially as compared to the wedge test. For example, even though the tensile strength tests gave equivalent results for the chemical

controls and the 60Al/40polyester plasma sprayed coatings, initial crack lengths in wedge tests were not equivalent with the highest performing adhesives. This discrepancy is attributed to lower strength of the room-temperature-curing adhesives used in the button pull tests. Consequently, because the initial crack length of a wedge test experiment and the locus of crack propagation are dependent on initial bond strength, we used these parameters to qualitatively evaluate dry (initial) tensile strength performance during most of the program. This procedure allowed one test to measure both initial tensile strength and bond durability. In principle, the initial crack length measurements could be converted to strength values.

Wedge tests were performed using Cytec FM-123, FM-300M, and FM-73 adhesives and 3M AF-163-2 adhesive. The FM-123 is a water-wicking adhesive that allows significant moisture to reach the bondline; however, it can also plasticize and reduce the stress at the crack tip. The FM-300M allows less moisture penetration, but gives a longer initial crack length and, hence, less initial stress. FM-73 gave performance for chemical controls and plasma sprayed surfaces similar to that of FM-123. Both scrim and mat support were used for the FM-73. No difference in the performance of the controls or plasma sprayed specimens was observed for the two varieties. The AF-163-2 showed only small differences in performance of FPL and PAA bonds – indicating an insensitivity to surface treatments. Although this behavior would be very important in production, it was not helpful in our developmental tests and this adhesive was seldom used.

Wedge test results for a 60%Al-Si/40%polyester plasma sprayed coating using Cytec FM-300M epoxy adhesive are given in Figure 2. For this adhesive, the plasma sprayed

coating gives crack growth very similar to that of PAA – the current state of the art in aluminum adherend surface treatments – as demonstrated by both the initial crack length (strength) and final crack length (durability). The locus of crack propagation under both dry and wet conditions was predominately within the coating for the plasma spray treatment. For PAA, the locus of failure was within the adhesive when dry and partially interfacial when wet. The similarity in performance suggests that the strength/toughness of the coating is very similar to that of this adhesive.

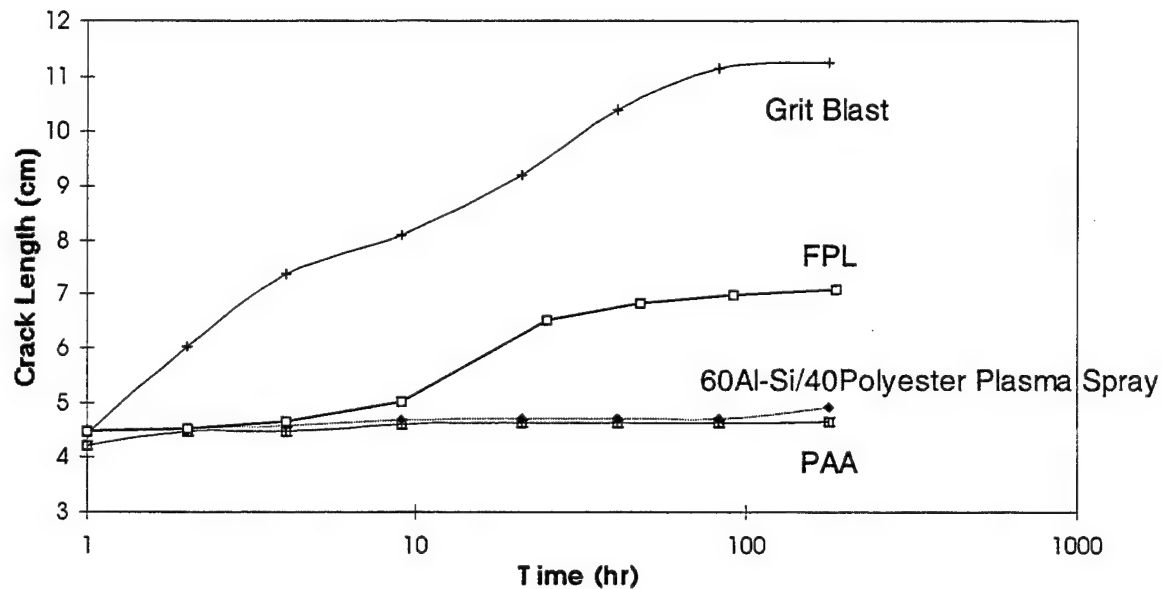


*Figure 2. Wedge test results for FPL, PAA, grit blast, and plasma sprayed 60AlSi/40polyester treatments for Cytec FM-300M epoxy adhesive.*

Also shown in Figure 2 is the performance of grit blasted adherends – a sometimes used nonchemical treatment for bonding. The durability of grit blasted joints is highly dependent on blasting procedures. The poor performance shown is representative of typical grit blasting operations. Under carefully controlled conditions, performance can

be improved to rival FPL performance, but further improvements are not feasible. The grit blasting treatment is suitable for applications requiring only moderate bondline strength or minimal exposure to moist conditions.

Wedge test results using all adhesives investigated are given in Figure 3 for the 60Al-Si/40polyester plasma sprayed coating. As before, for FM-300M, the plasma sprayed coating gives both initial and final crack lengths very similar to those of PAA. For FM-123, FM-73, and AF-163-2 the tougher adhesives exhibit a smaller initial crack length for the chemical controls for which propagation was cohesive within the adhesive. Because propagation for the plasma spray specimens is within the coating (see below), their initial crack lengths remain near those of the FM-300M specimens. Although crack growth for the plasma sprayed adherends is relatively small, similar to that for PAA, the initial crack length is greater than that of the controls so that the final crack length and hence the stress that the joint can withstand is intermediate between those of FPL and PAA.

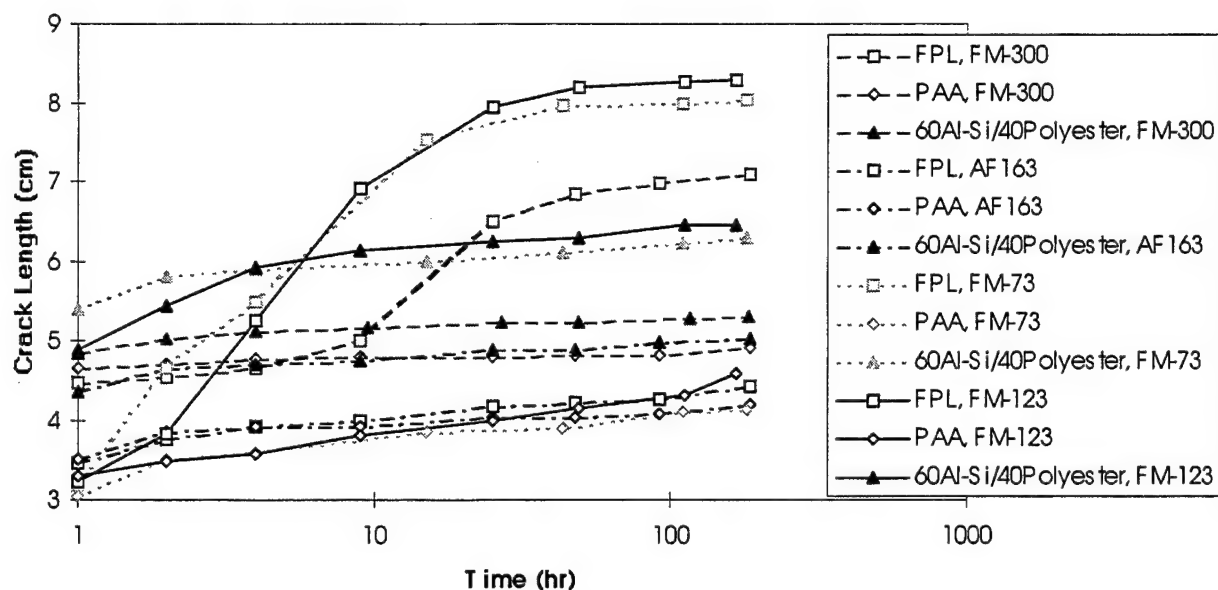
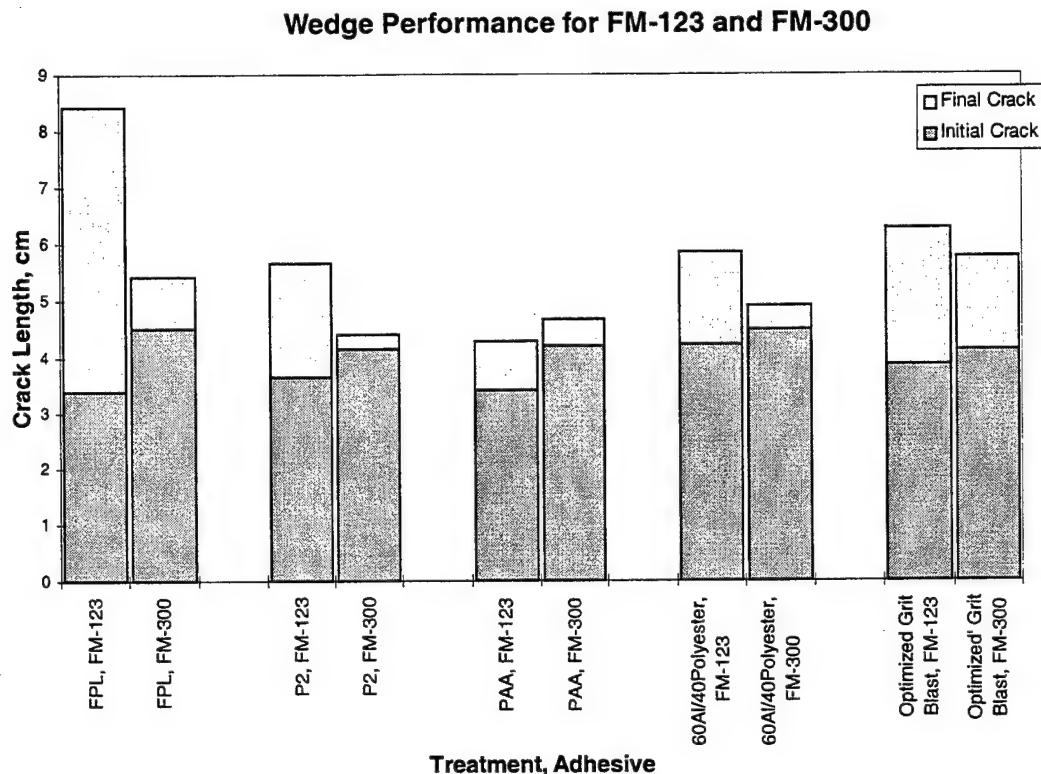


Figure 3. Wedge tests results for 60AlSi/40polyester plasma spray coating and FPL and PAA controls for Cytec FM-73, FM-123, and FM-300M and 3M AF-163.

The performances of the 60Al-Si/40polyester plasma spray and control treatments are compared for the FM-123 and FM-300M adhesives in Figure 4. The initial crack lengths for FM-123 adhesive were consistently less than those for FM-300M adhesive, especially for the chemical controls where the crack propagated initially within the adhesive. Each treatment showed reduced crack growth with FM-300M adhesive during humidity exposure, although the higher initial crack length for PAA caused the total crack length to be greater for this adhesive than for FM-123 adhesive.



*Figure 4. Comparison of initial and final crack lengths of 60(Al-Si)/40polyester plasma spray treatment and control treatments for FM-123 and FM-300M adhesives.*

The significantly lower crack growth during humidity exposure of the FPL and P2 specimens using FM-300M adhesive compared to FM-123 adhesive is likely an effect of lower moisture ingress in the former adhesive. Less moisture present at the bondline in advance of the crack tip means that hydration of the oxide is slowed. Thus, for surface preparations in which hydration is relatively rapid and moisture penetration to the bondline is the limiting factor (e.g., FPL and P2), significant improvements in crack growth can be obtained with the less water penetrable FM-300M adhesive. Nonetheless, it is surprising for the hydration of P2 to be slowed so much that the crack never reinitiates at the adhesive/substrate interface. For PAA, the hydration rate is slow enough that it is the limiting factor, rather than the time needed for moisture penetration to the bon-

dline.<sup>7,8,11-15</sup> Thus, little difference is observed in crack propagation for FM-123 and FM-300M adhesives. For the grit-blasted surface with its minimal physical bonding, crack growth is controlled by the moisture-induced breaking of secondary bonds. This process requires comparatively little moisture. In the 60Al-Si/40polyester case, crack propagation is through the coating. There may be some moisture effects in promoting crack growth in this case, e.g., a weakened AlSi/polyester interface or slow hydration of the aluminum (oxide), but the relative decrease in crack growth from FM-123 adhesive to FM-300M adhesive is less than that observed for FPL and P2 specimens.

Analysis of the surfaces formed during crack growth under dry conditions revealed that the crack propagated predominately through the polyester phase of the composite coating. This is demonstrated in the surface behavior diagram (SBD)<sup>14,16</sup> of Figure 5 where the Al, N, and C XPS atomic concentrations have been converted to Al-Si, adhesive, and polyester molar concentrations based on measurements from the adhesive, Al-Si, and polyester components. The SBD shows that crack propagated through a mixed interphase of the adhesive and the coating, but that the failure surface was polyester rich – that is, the composition falls to the left (polyester side) of the dashed line of stoichiometric composition. The penetration of the adhesive into the coating during cure was independently shown by specimens that had not been grit blasted prior to plasma spray and which failed at the adherend-coating interface. XPS analysis of the coating side of this interface clearly showed the presence of adhesive. The mechanism by which the adhesive penetrates into the coating is not known, but may involve microscopic porosity of the coating or a diffusion through the polyester during cure.

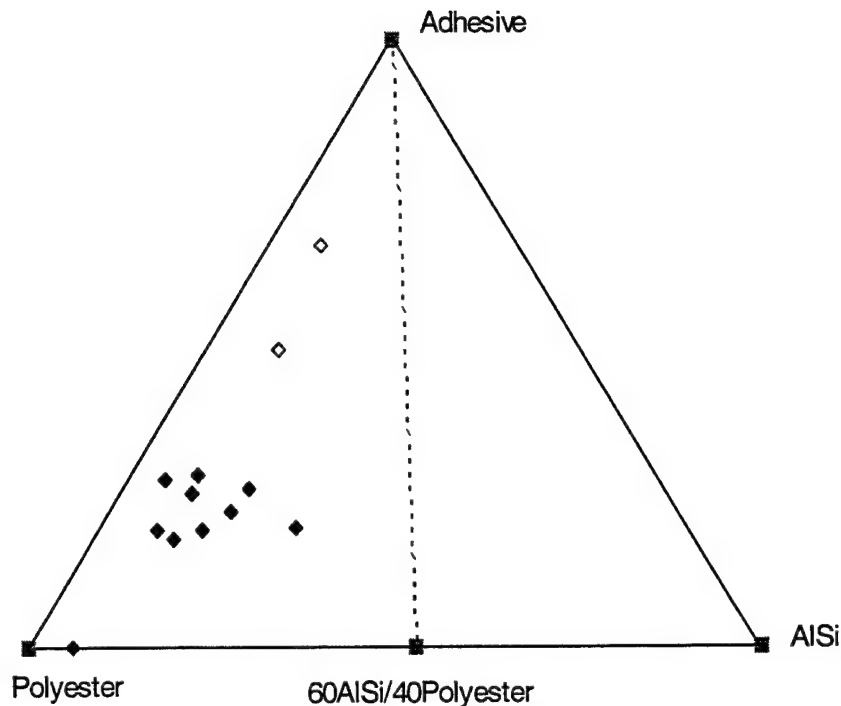


*Figure 5. Surface behavior diagram showing the locus of dry crack propagation of 60AlSi/40polyester wedge test specimens. The solid diamonds are the standard powder mix coatings; the open diamonds are the improved powder mix coatings (see below). The dashed line represents the 60/40 stoichiometric ratio.*

Four parameters were evaluated to improve performance: Al/polyester ratio, powder mixing, thickness, and polymer chemistry. Tests were performed using a range of coating composition, from 100% Al to 100% polyester as illustrated in Figure 6. The compilation of Figure 7 shows that initial crack length was optimized by a 80AlSi/20polyester ratio and crack propagation. In many cases, failure for this composition occurred within the adhesive unlike the other compositions which generally failed within the coating. However, the best durability was achieved by the 60AlSi/40polyester blend. The poor performance observed for the 70AlSi/30polyester coating is surprising consid-

ering the other results. The experiments were repeated with equivalent results. Incomplete mixing or component separation is believed to have contributed to the poor performance. The two single-component coatings (polyester and aluminum) exhibited poor performance with large initial crack lengths. Crack propagation appeared to be at the coating/metal interface, suggesting that the two components synergistically promote adhesion to the substrate. Because the best performance was shown by the 60AlSi/40polyester blend, most of the effort concentrated on this composition.

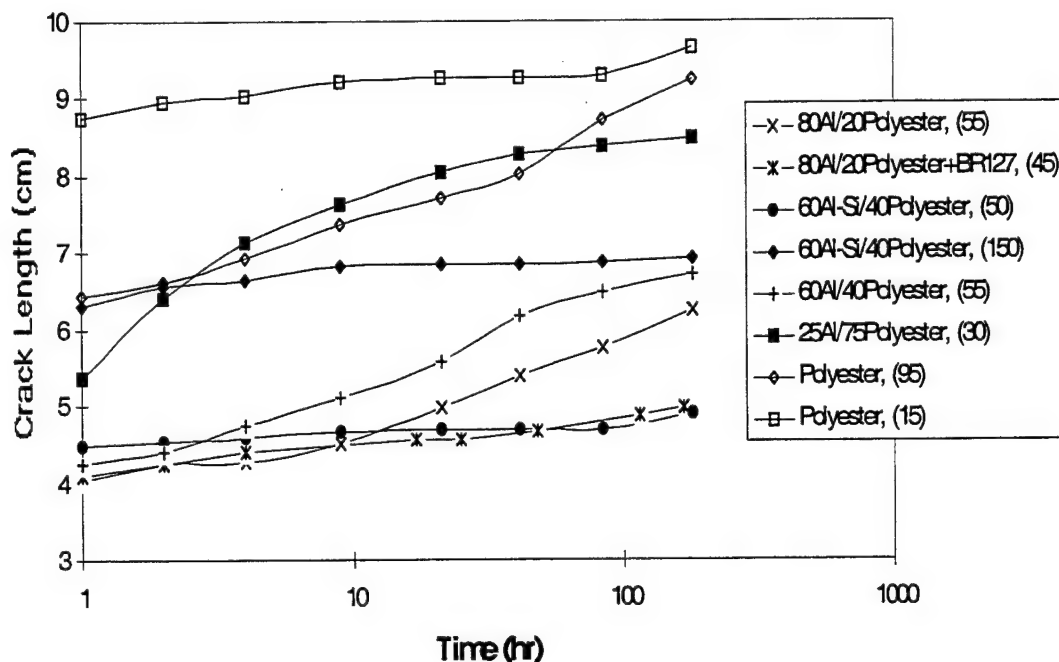


Figure 6. Wedge test performance of Al/polyester and pure polyester treatments using FM-300M adhesive. The numbers in parentheses are the thickness of the plasma sprayed coating in  $\mu\text{m}$ .

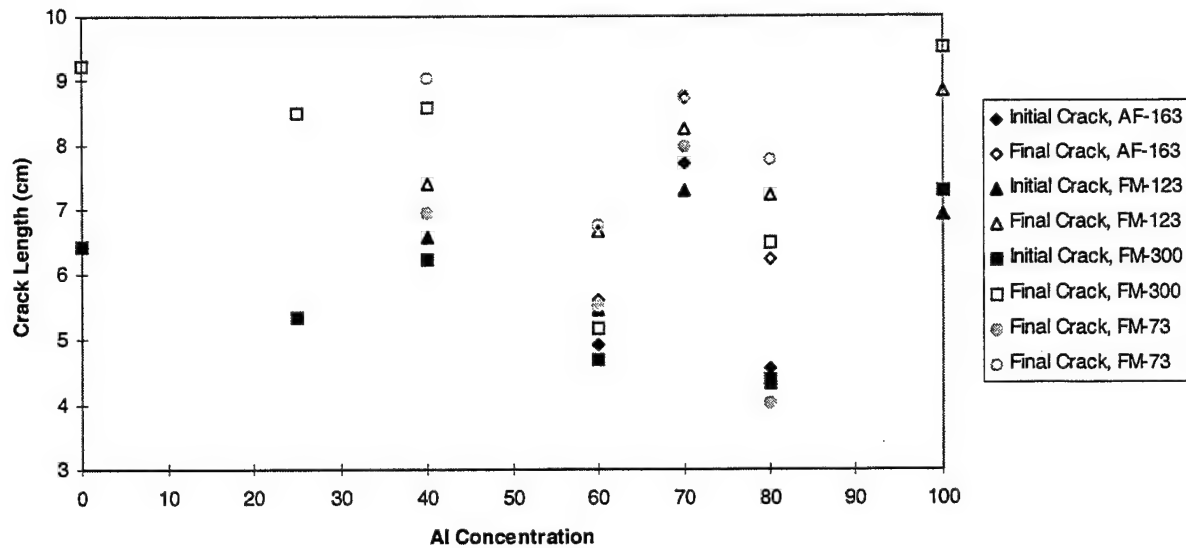
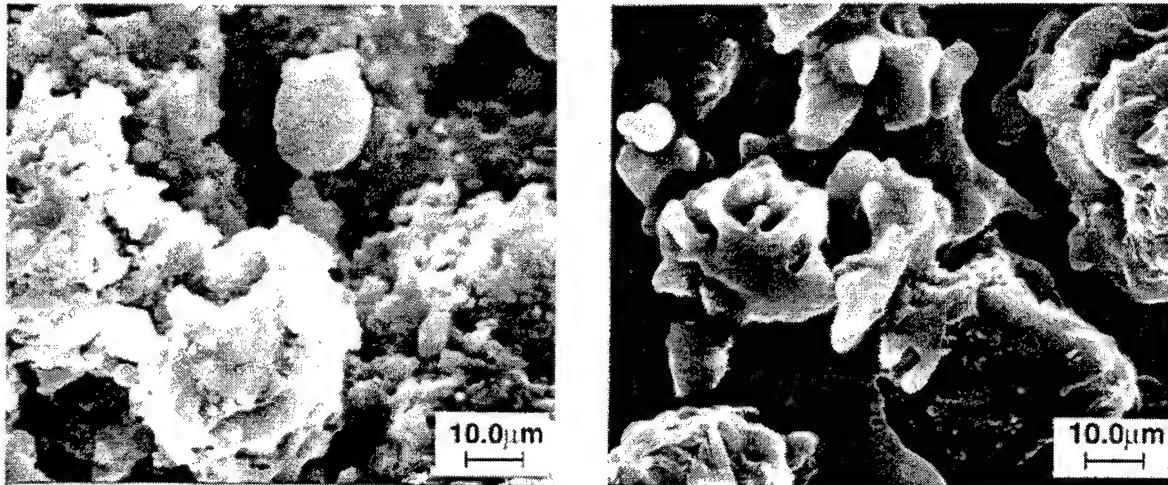


Figure 7. Average initial and final crack lengths as a function of AlSi concentration for wedge tests using plasma sprayed AlSi/polyester coatings and the four adhesives. The number of tests included in the average vary considerably: concentrations with AlSi concentrations less than 30% were evaluated only once; the 60AlSi40polyester was evaluated in over 30 experiments.

Electron micrographs (Figure 8) of selected coatings prior to bonding showed that the surfaces were convoluted on a moderate microscopic scale (1-10  $\mu\text{m}$ ). The roughness is very irregular and over a wide range of scale suggesting good opportunities for mechanical interlocking. Nonetheless, compared to the pores and whiskers of PAA or FPL surfaces,<sup>17,18</sup> there is less fine-scale structure and hence a lower density of potential physical bonds (Figure 9). Consequently the number of physical bonds (mechanical interlocks) is reduced over the chemical controls although the larger physical bonds present will individually be stronger. The penetration of the adhesive into the coating suggests good interphasal strength. Failure modes ranged from within the adhesive

(some 80AlSi/20polyester bonds) to within the coating (60AlSi40polyester and some 80AlSi/20polyester bonds) to the coating/metal interface (low and high Al coating content). Collectively, these failure modes suggest a strong adhesive/coating interphase.



*Figure 8. SEM micrographs of 60AlSi/40polyester and 100Al plasma sprayed surfaces prior to bonding.*

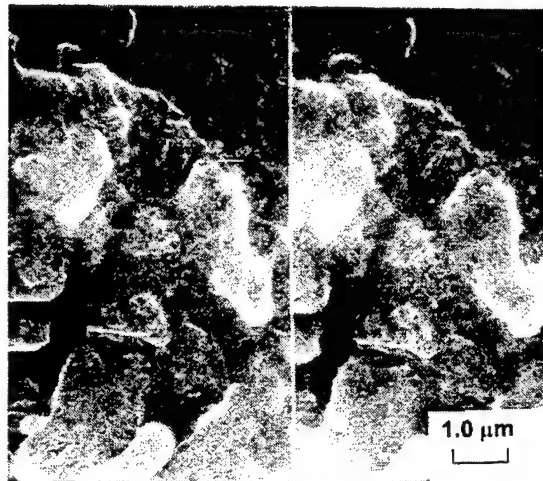


*Figure 9. SEM micrograph of 60AlSi/40polyester surface prior to bonding. Compared to FPL and PAA surfaces, little small scale microroughness is present.*

Often the thickness of a coating or other thin film is an important factor in coating properties, including strength. Thicker coatings generally are weaker and provide an easier path for crack propagation. A compilation of results (Figure 10) over a range of 60AlSi/40polyester coating thicknesses revealed that optimum final crack length is obtained with a thickness of 50-75  $\mu\text{m}$  (2-3 mils) which was our nominal thickness for most of the program. Although the initial crack length was improved at thinner coatings, extrapolating to zero thickness would still give initial crack lengths greater than those of the chemical controls (3.0-3.5 cm). The considerable scatter indicates that other factors besides coating thickness are also important in determining bond performance. However, these factors do not include the choice of aluminum substrate alloy; no significant difference is seen between 2024-T3 and 7075-T6. Such independence of alloy is not surprising. Because the plasma spray operation deposits a coating physically without any chemical reaction with the substrate, the substrate material has a much smaller effect on the coating and coating adhesion than the case of a conversion coating or other chemically formed coatings.

Surface analysis of the dry failure surfaces showed that the crack propagated in the coating-adhesive interphase region, but predominately in the polyester phase of the coating for all compositions (Figure 11). The only significant exceptions are the trivial case of 100AlSi where there is no polyester and some of the 80AlSi/20polyester specimens where failure was within the adhesive, as previously noted.

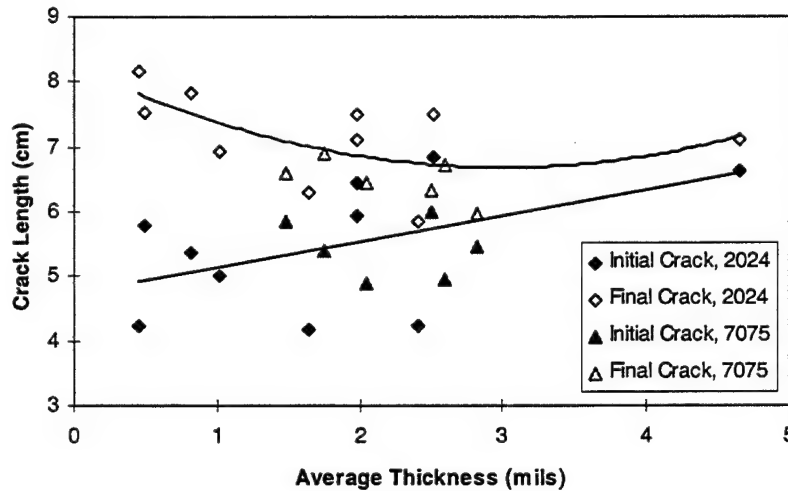


Figure 10. Initial and final crack lengths for wedge test specimens with 60AlSi/40polyester coatings as a function of coating thickness. The adhesive is Cytec FM-123. Also shown is the negligible effect of alloy on performance.

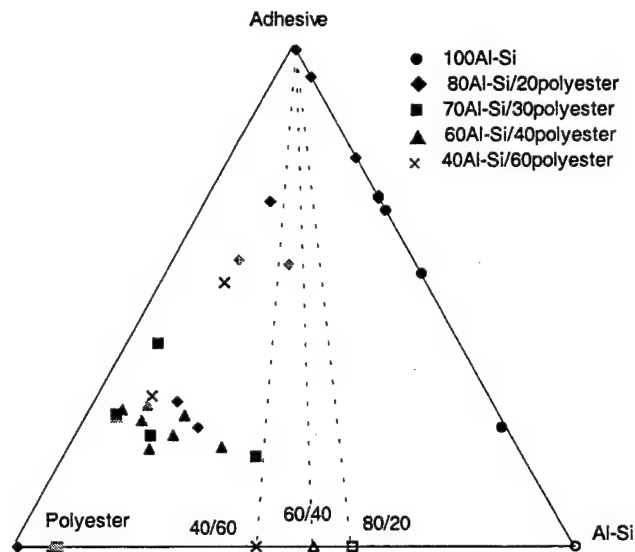


Figure 11. SBD showing dry failure surfaces of wedge tests for several AlSi/polyester coating compositions. All four adhesives are represented here, no significant difference in failure mode was seen for the different adhesives. The dashed lines correspond to stoichiometric lines of 40AlSi/60polyester, 60AlSi/40polyester, and 80AlSi/20polyester.

The extent of the polyester phase present on the dry failure surfaces suggested that the coating had larger regions of the two phases than expected; that is, the coating was heterogeneous on a larger scale than predicted from random mixing of the two components. To reduce electrostatic charging and clumping of the powder during mixing and handling, it was blended, sieved, and chopped several times. The equipment was carefully grounded as was the spray hopper. A wire was inserted in the feed line to the spray gun to further reduce electrostatic charging. This procedure resulted in a more homogeneous coating that showed improved initial crack length that was closer to that of the controls, but still somewhat longer (Figure 12). The final crack length was also improved, indicating that the joint could withstand greater stress even after humidity exposure. XPS showed the crack propagated within the interphase region where the coating and the adhesive are mixed together with approximately 50% propagation within the adhesive. However, within the coating, the crack still predominately traveled through the polyester phase (Figure 5). Based on these results and the apparent propensity for the AlSi/polyester powder grains to charge and clump together, it is believed that some of the scatter and variability shown in the initial and final crack lengths (see, e.g., Figure 10) is a result of poor mixing and large scale inhomogeneity of the coating. For example, the extent of charging would be dependent on the relative humidity during powder mixing and spraying. The sensitivity of the coating performance to such factors would be a consideration for production as it would require increased process controls.

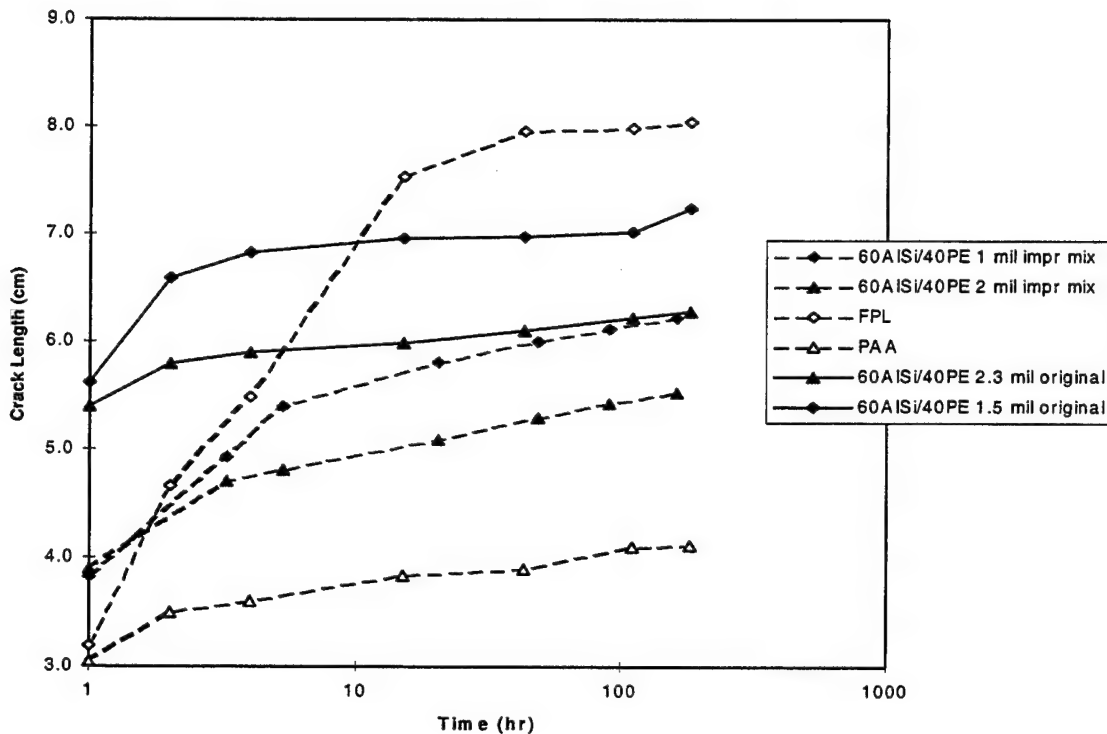


Figure 12. Wedge test results comparing original and electrostatic reduced mixing of 60%AlSi/40%polyester. Also shown are the FPL and PAA controls. The adhesive was Cytec FM-73. The coating with the reduced electrostatic charging was prepared by the second plasma sprayer (PS#2).

Combinations of aluminum and PEEK (polyetheretherketone) were also evaluated, but to a much lesser extent (Figure 13 and Figure 14). Because PEEK is a commonly sprayed polymer, used for adhesion in bone implants, among other applications, it might have been expected to improve the toughness of the composite coating. However, the behavior is very similar between Al/polyester and Al/PEEK coatings. Both give comparable performance at 60%Al composition. Both exhibit very poor performance of the pure polymer coating with failure between the coating and the substrate. Apparently one role of the aluminum is to enhance adhesion to the metal.

The superior performance of the aluminum/polymer blends compared to the individual components demonstrates the synergism between the constituents. The aluminum is necessary to obtain proper adhesion to the substrate as the impacting aluminum particles embed themselves into the base metal. Without this aluminum anchor, the pure polymer coatings fail at the coating/metal interface. Although the aluminum provides the structural framework for the coating, some polymer is needed for toughness. Without polymer, the crack propagates through the aluminum coating more easily. Nonetheless, failure was predominately through the polyester phase of Al/polyester coatings.

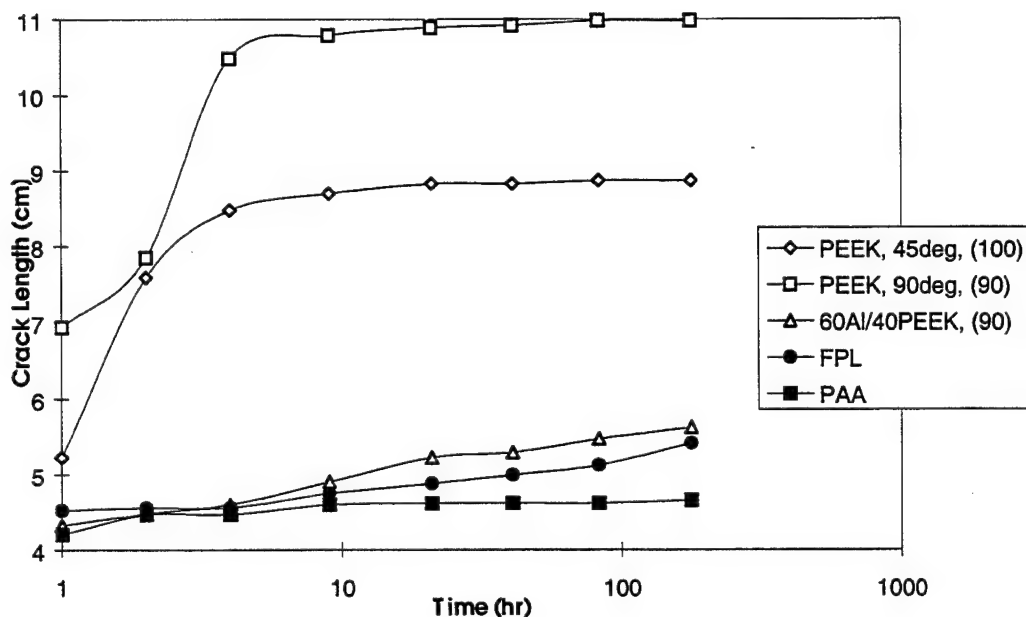


Figure 13. Wedge tests results for plasma sprayed PEEK and 60Al/40PEEK coatings and FPL and PAA controls. The adhesive was Cytec FM-300M. The numbers in parentheses are the coating thicknesses in  $\mu\text{m}$ .

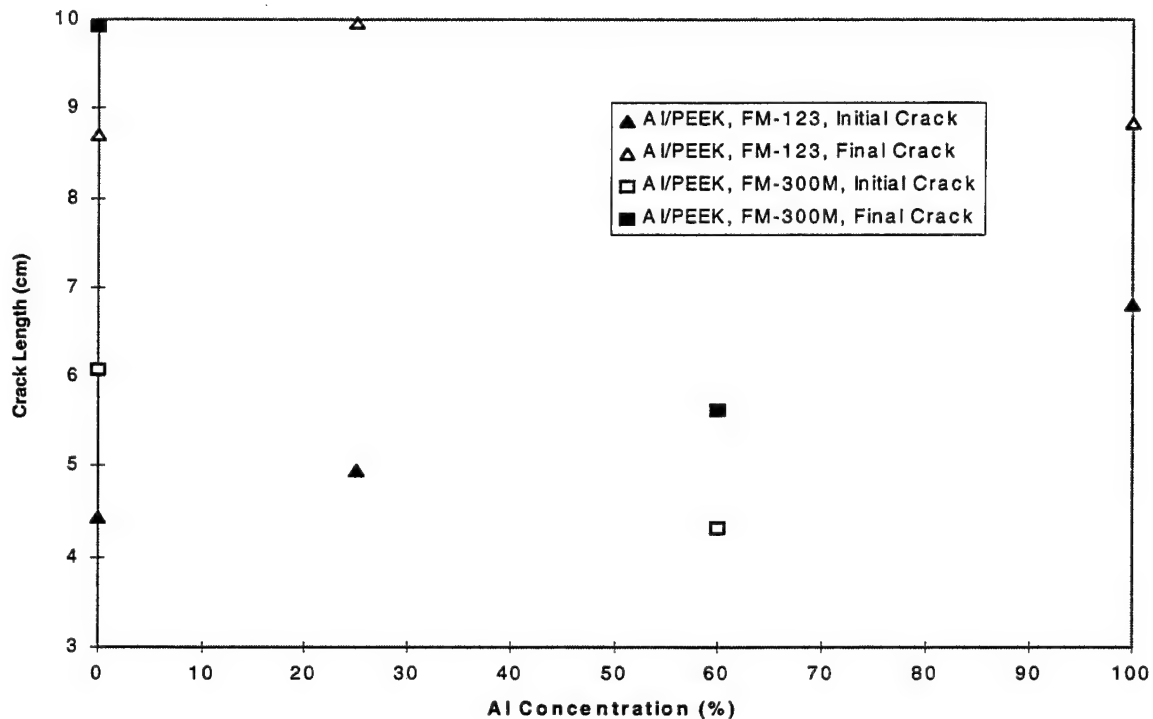


Figure 14. Initial and final crack length results as a function of Al concentration for wedge test specimens with plasma sprayed Al/PEEK coatings.

The physical bonding occurs over relatively large scales as indicated by the interpenetration of the adhesive into (and in some cases through) the coating. Sufficient interconnected porosity is present to allow migration of the adhesive during the early curing stage. As such, the adhesive reinforces the coating and enhances the coating/adhesive bond. Interconnected porosity is common to plasma-sprayed coatings, especially for ones as thin as investigated here. Pike et al. reported that 8-10% porosity was needed to obtain adequate physical bonding for their alumina coatings.<sup>2</sup> To obtain a sufficient moisture barrier to prevent substrate corrosion of plasma-sprayed steel exposed to high humidity, a Ni-Cr coating of 150-250  $\mu\text{m}$  was needed. To protect against the more severe environment of alternate immersion in salt water, even coatings of up

to 450  $\mu\text{m}$  had sufficient interconnected porosity to require supplemental cathodic protection to prevent corrosion of the steel.<sup>5</sup>

### **3.1.2 Titanium and Other Metal Coatings**

To eliminate the weak polyester component of the composite coatings, all metal coatings were evaluated. Titanium (Ti-6Al-4V) coatings gave the best performance. Figure 15 shows the best results with initial and final crack lengths matching that of PAA. Dry crack propagation was within the adhesive while propagation under humid conditions was interfacial between the adhesive and the coating. (A similar locus of failure was observed for unprimed PAA.) Unlike the 100%Al coating, the coating-substrate bond appeared stronger than the coating and the adhesive. For wedge test 96-11, the initial crack length was significantly shorter than any other specimen. The increased stress was sufficient to bend the aluminum adherends.

Because parallel wedge tests involving plasma sprayed Ti-6Al-4V coatings on Ti-6Al-4V adherends had exhibited entirely cohesive crack propagation using Cytec FM-300M adhesive (see Table 3), it is believed that further improvements are possible. However, despite the initial, very promising success, attempts to improve performance and obtain completely cohesive crack propagation did not achieve their goals. The subsequent data are shown in Figure 16. Crack propagation under dry conditions was predominately in the adhesive. Propagation under moist conditions was predominately interfacial between the adhesive and the coating.

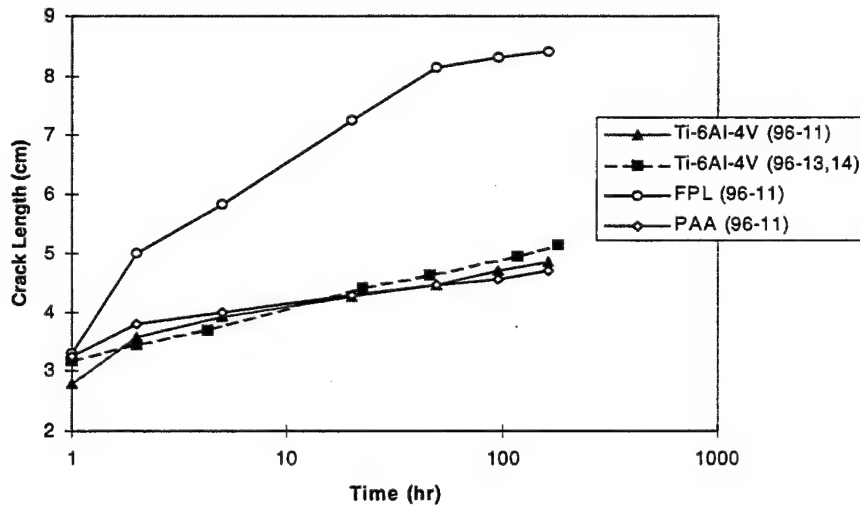


Figure 15. Wedge test results for Ti-6Al-4V coatings on 2024 Al compared to PAA and FPL controls. The adhesive is Cytec FM-73. The data represent two pairs of panels sprayed at the same time, but bonded separately and tested over three wedge tests. Data for wedge test 96-11 do not include two specimens – one showed poor performance and failure within the coating; the other (adjacent) specimen showed intermediate performance and partial coating failure.

Performance is independent of thickness in the range of 12-50  $\mu\text{m}$  (0.5-2 mils). It is independent of whether the aluminum is cut into 2.5x15-cm (1x6-in.) strips before spraying or after bonding. Despite several attempts, including various plasma spray parameter settings and two-wire arc spraying, a second spray company could not duplicate the performance shown in Figure 15. However, the first spray company did not reproduce the results despite nominally identical operating conditions. SEM characterization (Figure 17) showed similar “large” scale roughness (features > 1 $\mu\text{m}$ ) on the two sets of specimens, but a finer scale roughness (features < 1 $\mu\text{m}$ ) on the specimens of Figure 15 compared to the specimens of Figure 16. Fine scale microroughness has

previously been identified as critical to achieving excellent bond durability.<sup>17,19</sup> The very high density of physical bonding (mechanical interlocking) assures high interfacial strength and durability. In the case of a titanium surface where the surface is stable and does not change chemistry or morphology under these conditions, the density of physical bonds is the controlling factor in bond performance. A different lot of titanium powder was used for the two sets of specimens. Previous plasma spray coating evaluations have observed coating property variations with changes in vendor supplies or operations. The rapidly changing market in titanium may have been a factor in the change in performance.

For many of the bondments, there were areas of coating failure – crack propagation within the coating or interfacially between the coating and the substrate. In most cases, these were small isolated areas, often along the edge of the specimen. Once, it was the entire specimen (20% of the 15x15-cm (6x6-in.) panel). Small areas did not seem to affect the bond performance. These findings suggest a nonuniformity in the coating that would need to be resolved during further development.

To evaluate the need for a primer to improve wetting of the substrate, limited experiments were performed using brush-coated Cytec BR-127 (Figure 18). Significant improvement was observed with the primer, but performance did not match that of PAA. The locus of failure was within the primer as indicated by significant levels of Cr on both sides as determined by XPS. We believe that a thinner primer coating would have given less crack length. Under a National Rotorcraft Technology Center/Rotorcraft Industry Technology Association (NRTC/RITA) funded program, we obtained better results (comparable to PAA) by using an adhesive primer prior to bonding. Because the

Ti coating passivates or stabilizes the aluminum surface (see corrosion results below), the primer would serve more to improve wetting of the surface than to protect the surface from hydration/corrosion.

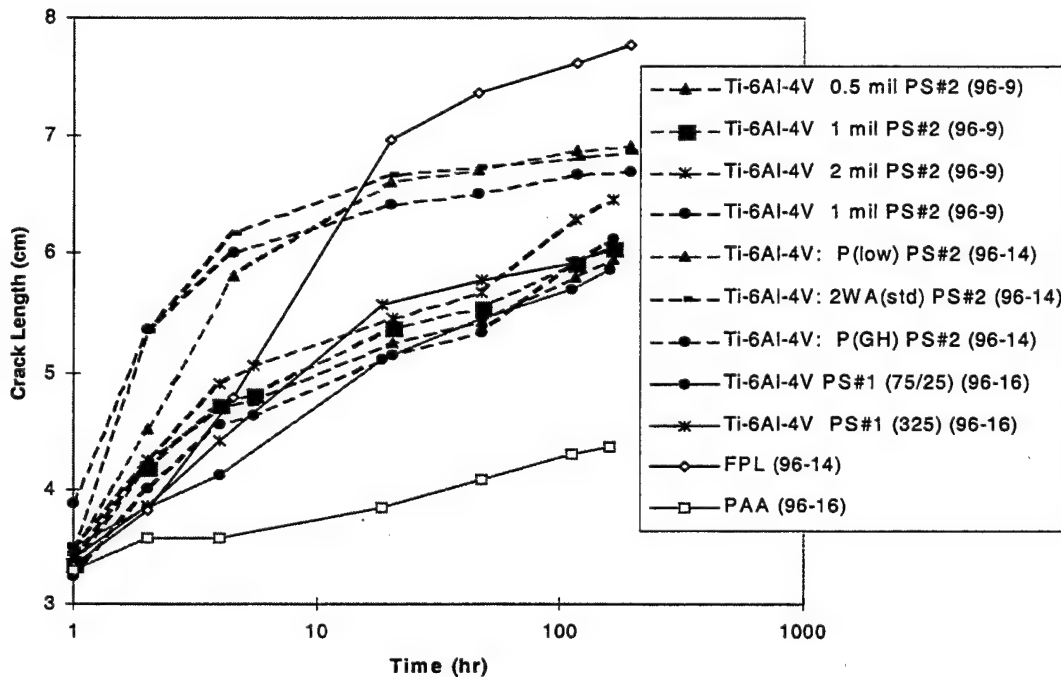


Figure 16. Wedge tests results for subsequent Ti-6Al-4V coatings on Al. The adhesive was Cytec FM-73. Unless otherwise noted, the thickness was nominally 2 mils. The wedge test (96-\*) and sprayer are given in the legend. One of the specimens was sprayed using the two-wire arc process. The 325 indicates a powder mesh size of -325 (the same as that of Figure 15). The 75/25 indicates a powder mixture of 75% -325 and 25% 150.

The use of non-aluminum coatings (titanium and nickel/aluminum, below) introduces concerns about galvanic attack, i.e., corrosion induced because of the electrochemical differences between the two metals. To determine if corrosion rates were increased because of the plasma sprayed coatings, the rates were measured using Tafel slopes

from potentiodynamic polarization. The corrosion rates in 5.0% NaCl solutions are given in Table 2. The data show the Ti passivates the aluminum surface. Although one would anticipate the titanium to induce corrosion of the aluminum, this does not occur. We hypothesize that the TiO<sub>2</sub> film on the Ti serves to isolate the Ti and Al and prevent or at least significantly reduce galvanic effects.

*Table 2. Corrosion Rates of Thermally Sprayed Aluminum*

<i>Composition</i>	<i>Spray Procedure</i>	<i>Thickness</i>	<i>Condition</i>	<i>Exposed Surface</i>	<i>Corrosion Rate</i> (mil/yr)
Ti6Al4V	Plasma	2 mils	Normal	Ti6Al4V	1.6
Ti6Al4V	Plasma	2 mils	Low Power	Ti6Al4V	0.59
Ti6Al4V	two-wire arc	2 mils	Normal	Ti6Al4V	3.5
Ti6Al4V	Plasma	0.5 mils	Normal	Ti6Al4V and Al	2.1
Ti6Al4V	Plasma	2 mils	Normal	Ti6Al4V and Al	2.0
bare substrate	-	-	sanded		18.1

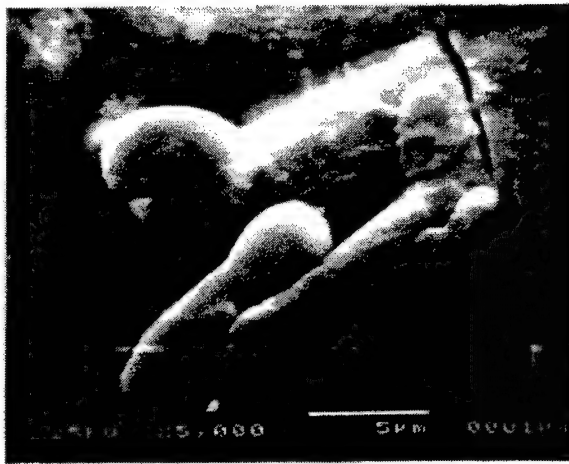
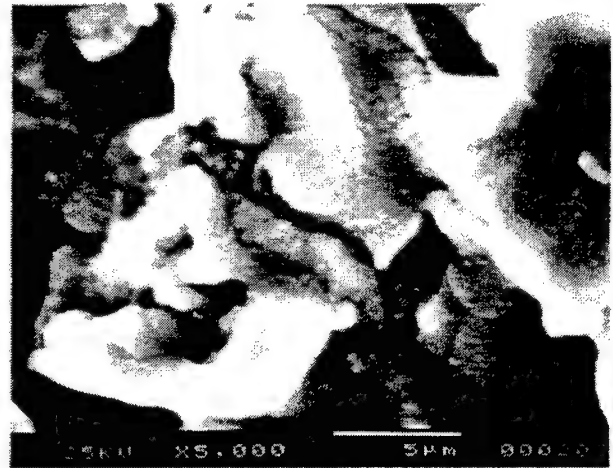
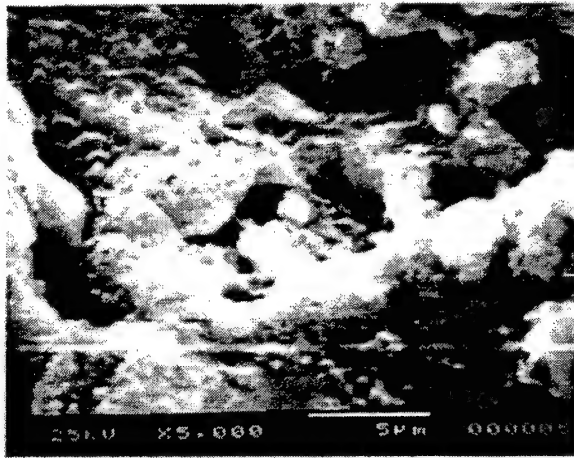


*Figure 17. SEM micrographs of Ti-6Al-4V coated aluminum. Upper left, 96-11 specimen (PS#1) showing excellent bond durability in Figure 15. Upper right, 96-16 specimen (-325 mesh, PS#1) showing moderate bond durability in Figure 16. Lower left, 2-mil 96-9 specimen (PS#2) showing moderate bond durability in Figure 16. Lower right, 96-14 specimen (low power plasma, PS#2) showing poor bond durability in Figure 16.*

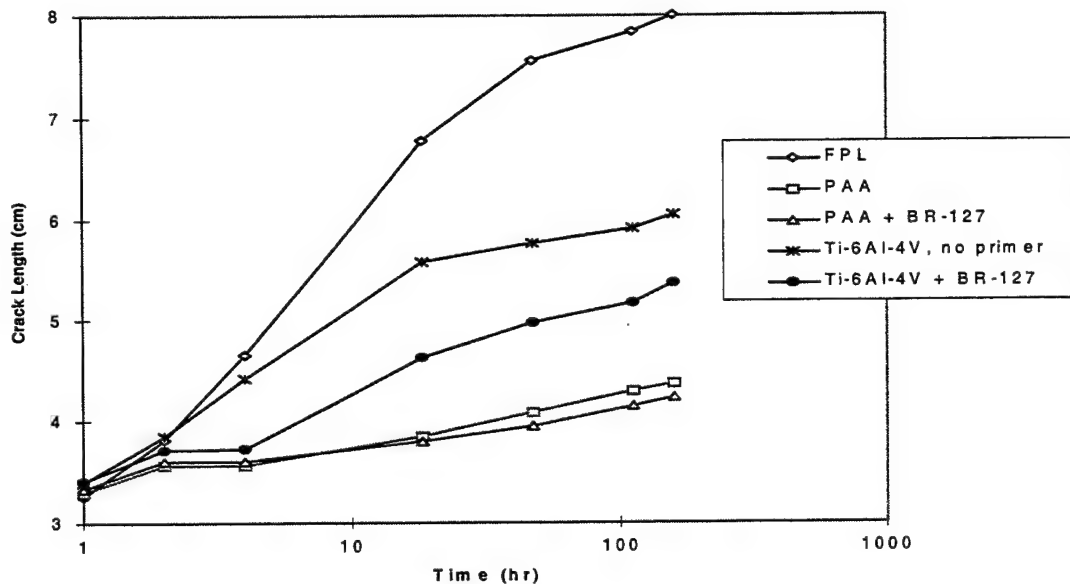


Figure 18. Wedge tests results showing the effect of Cytac BR-127 primer. The adhesive was Cytac FM-73. Specimens were prepared by PS#1.

Nickel/aluminum coatings were also evaluated as all-metal coatings. Both plasma and two-wire arc spray were used for deposition (Figure 19). Dry crack propagation occurred predominately through the adhesive, reflecting the increased toughness of coating exhibited by the metallic coatings. One plasma-sprayed joint failed partially at the interface and this locus of failure resulted in a larger initial crack length. Performance during humidity exposure was not as good as that of the best titanium coated specimens. There was rapid crack growth during the first hour of exposure. At the end of the wedge test, final crack lengths were comparable to that of FPL specimens. No significant difference was seen between the plasma and two-wire arc sprayed specimens.

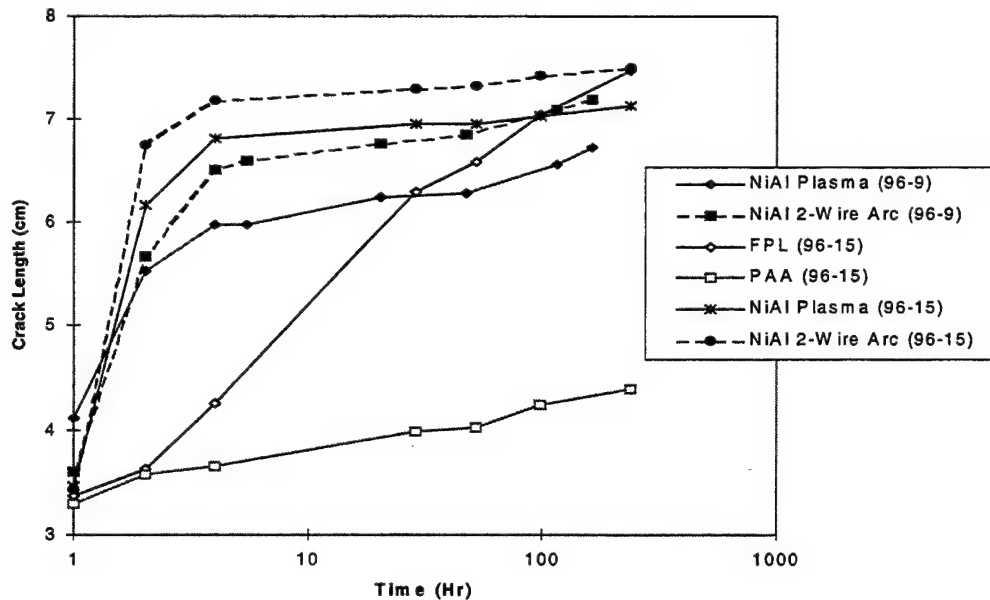


Figure 19. Wedge tests results for plasma sprayed and two-wire arc sprayed Ni/Al coatings compared to the chemical controls. The adhesive was Cytec FM-73. The numbers in parentheses identify the specific wedge test. Specimens were prepared by PS#2.

SEM micrographs (Figure 20) show a moderate amount of microscopic roughness that should have prevented the very rapid crack growth upon humidity exposure, but not necessarily the slow crack growth observed for the titanium coated specimens. The discrepancy may be explained by three possibilities: 1) The area from which the micrographs were taken was not representative of the majority of the surface; 2) Complete wetting of the surface may not have occurred; 3) Corrosion of the coating disrupted the physical bonding with the adhesive and induced additional stress from the increased volume of corrosion products. The first hypothesis cannot be proven or disproven at this time, but generally these surfaces have been reasonably uniform. The similarity between micrographs of the plasma and two-wire arc sprayed surfaces argues

against this hypothesis. Corrosion products were visibly present on the wedge test wet failure surfaces following post-test separation. Electrochemical corrosion rate measurements using Taffel slopes indicated that the NiAl provided no protection from corrosion compared to uncoated aluminum (Table 2). Regardless of the reason, the performance of these coatings was not good in these experiments. However, it is interesting to note that when these coatings were investigated in a separate program using a primer (Hysol EA9210H) and different adhesive (Hysol EA9628) , the performance was nearly equivalent to that of PAA.



*Figure 20. SEM micrograph of plasma sprayed NiAl coating (PS#2).*

### **3.1.3 Alumina**

Alumina coatings were one of our initial plasma spray treatments. Unlike the amorphous,  $\gamma$ - $\text{Al}_2\text{O}_3$ -like oxide formed during etching or anodization that hydrates readily, the  $\alpha$ - $\text{Al}_2\text{O}_3$ -like coating deposited by plasma spraying was expected to be more stable. Hydration experiments showed this hypothesis to be true. Coupons with a plasma sprayed alumina coating did not hydrate in boiling water even after 3 hours while grit blasted, FPL, and PAA surfaces hydrated within minutes.

Tensile button tests (Figure 1) exhibited failure within the coating at a lower strength than the chemical controls or the aluminum-polyester coatings. Early wedge tests using alumina coatings showed very poor results (Figure 21). The initial cracks were very long, with propagation in the coating below the interphase region where the adhesive migrated into the alumina. Adding 25% aluminum to the coating had no effect on the toughness of the coating. Because the coatings were so brittle and the aluminum/polyester coatings were more promising, the alumina coatings were not further evaluated during most of the program.

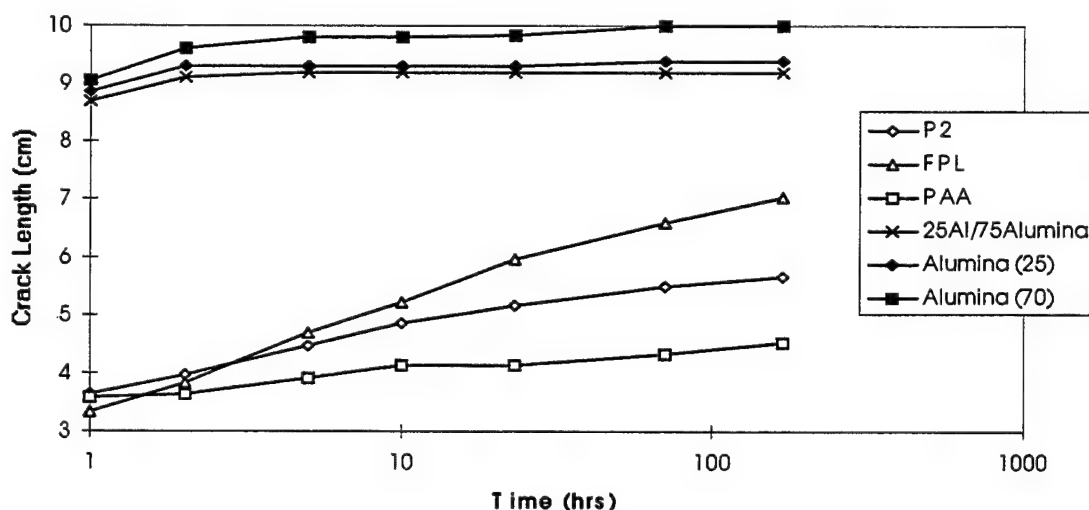


Figure 21. Early wedge test results for alumina and alumina/aluminum plasma sprayed coatings. The numbers in parentheses correspond to the thickness in micrometers. The adhesive was Cytec FM-123. Specimens were prepared by PS#1.

Despite our lack of success with alumina coatings, Dillard and co-workers<sup>3,4</sup> and Pike and co-workers<sup>2</sup> reported excellent results with alumina-coated aluminum. Therefore, toward the end of the program, we reevaluated alumina coatings. By this point, we had established a working relationship with the coating company which had performed the

plasma spraying of alumina for the Dillard and Pike groups. The wedge test results are presented in Figure 22. Improvement in the joint toughness is readily seen – under dry conditions, the crack propagated through the adhesive and not the coating. However, upon humidity exposure, the crack propagation shifted to the adhesive-coating interface. Under moist conditions, this interface gave little resistance to crack propagation and little stress was withstood by the joint at the end of the experiment. When the 50  $\mu\text{m}$  (2 mil) specimens were separated after the wedge test, some areas exhibited cohesive failure within the coating although none exhibited this locus of failure during the initial driving of the wedge.

SEM micrographs (Figure 23) showed the surface to be relatively smooth without much opportunity for mechanical interlocking. Nonetheless, the existing physical bonds (mechanical interlocking) and secondary chemical bonds between the adhesive and the alumina are sufficient to promote cohesive failure of the adhesive under dry conditions. The second coating (Figure 22) itself is certainly stronger than initial coating (Figure 21). However, once moisture disrupts the secondary chemical bonds, the interface is an easy path for crack propagation.

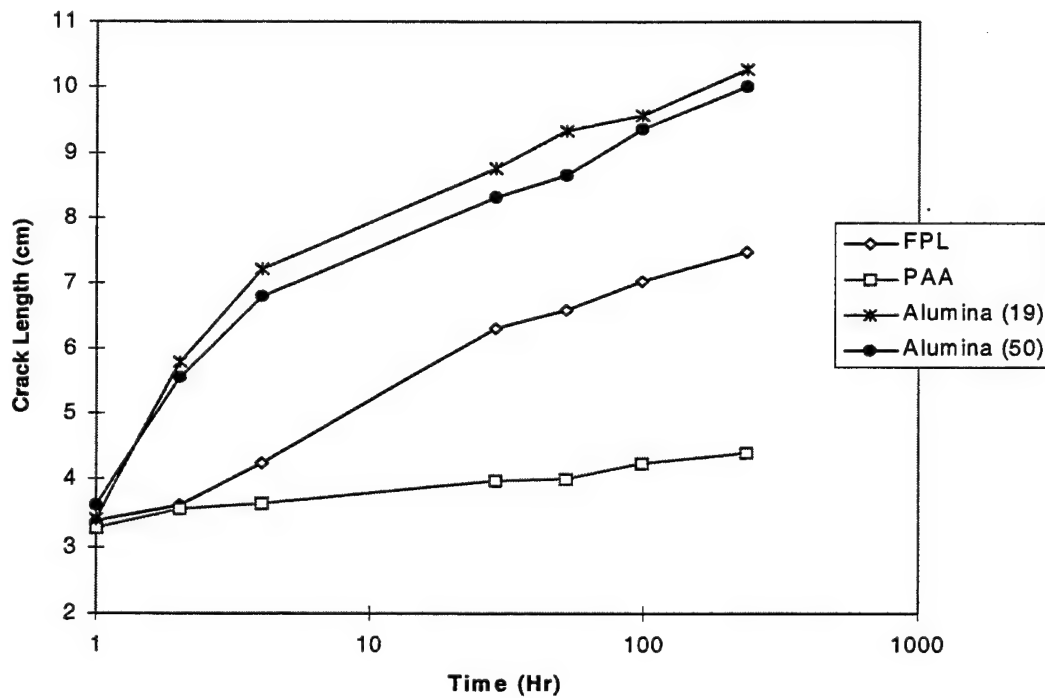


Figure 22. Wedge test results for plasma sprayed alumina specimens compared to chemical controls. Thicknesses are given in parentheses in micrometers. Adhesive was Cytec FM-73. Specimens were prepared by PS#2.



Figure 23. SEM micrograph of 2-mil  $\text{Al}_2\text{O}_3$  coating showing little opportunity for mechanical interlocking. Specimen was prepared by PS#2.

The poor performance of our alumina coatings is in contrast to the results of Pike et al.<sup>2</sup> and Dillard and Wolfe.<sup>3,4</sup> Pike et al. reported that plasma-sprayed alumina treatment gave equivalent performance to PAA treatment in compressive lap shear and wedge tests. Dillard and coworkers have shown that alumina and other ceramic coatings also give wedge test and butt torsion test performance similar to PAA. Both groups deposited 25 to 50- $\mu$ m-thick coatings. The reasons for these differences are not known; different adhesives were used in each case, but it is not expected that adhesive-dependent behavior would be that marked. One possible explanation is variations in the nature of the alumina coating. The plasma spray conditions/operator clearly make a difference as reflected in comparing Figure 21 and Figure 22. However, our later experiments used the same operator and supposedly the same spraying conditions as the other two groups. If slight and uncontrolled variations in the coating produce very differing bond performance, clearly processing controls would need to be very stringent to assure reliability. The more likely explanation is differences in the experimental conditions. We used standard wedge test conditions with condensing ( $\sim 98\%$ RH) moisture — conditions used by Boeing to correlate wedge test performance with service performance.<sup>20,21</sup> The cyclic wedge test conditions by the Dillard group are not standard and it is unknown how they compare in severity with our conditions. One could argue that cyclic conditions are well known to be more damaging or stressful than static conditions. On the other hand, the short (2 or 24 hr), lower (70%RH) humidity exposure in the Dillard experiments may not allow equilibration and hydration incubation times to occur. Once the specimens are removed from the humidity and dried, the specimens recover and humidity effects must begin anew. It is likely that the relative importance of these

effects and, hence, the severity will depend on surface treatments and other parameters. Pike et al. did not give sufficient experimental details to compare their conditions with ours so we cannot speculate on how their experiments and findings differ.

### **3.2 Titanium Adherends**

Previously reported pull strength measurements showed that plasma-sprayed Ti-6Al-4V coatings gave results identical to CAA and sodium hydroxide anodization (SHA) treatments at room temperature and moderately elevated temperatures.<sup>1</sup> Failure was within the epoxy adhesive. For specimens exposed to high temperatures (400-1200°C) prior to bonding, the plasma-sprayed specimens continued to provide high bond strength with cohesive failures. In contrast, CAA-treated specimens failed interfacially (oxide/metal) at very low strengths. At high temperatures, the oxygen in the CAA oxide dissolves or diffuses into the titanium substrate. This dissolution embrittles the metal and creates vacancies and voids that weaken the oxide – both effects serve to promote interfacial failure.

In this program, we initially tested two different thicknesses of plasma-sprayed Ti-6Al-4V coatings onto Ti-6Al-4V and compared them to several control treatments. The wedge test results are given in Figure 24 and the loci of failure given in Table 3. The better plasma spray treatment (50  $\mu\text{m}$ , 45°) gave final crack extension identical to that of the best chemical controls (CAA and Turco 5578) and better than that of Pasa-Jell 107. Propagation was entirely within the adhesive for both the plasma spray and CAA specimens but was interfacial for the Turco and Pasa-Jell. Such loci of failure are consistent with morphological considerations as reported earlier.<sup>17,22</sup> The optimized grit

blasting process gave reasonable, but not excellent, performance. This behavior again showed the strong dependence on blasting parameter; previous tests using conventional grit blasting exhibited very rapid and extensive crack growth.<sup>1</sup>

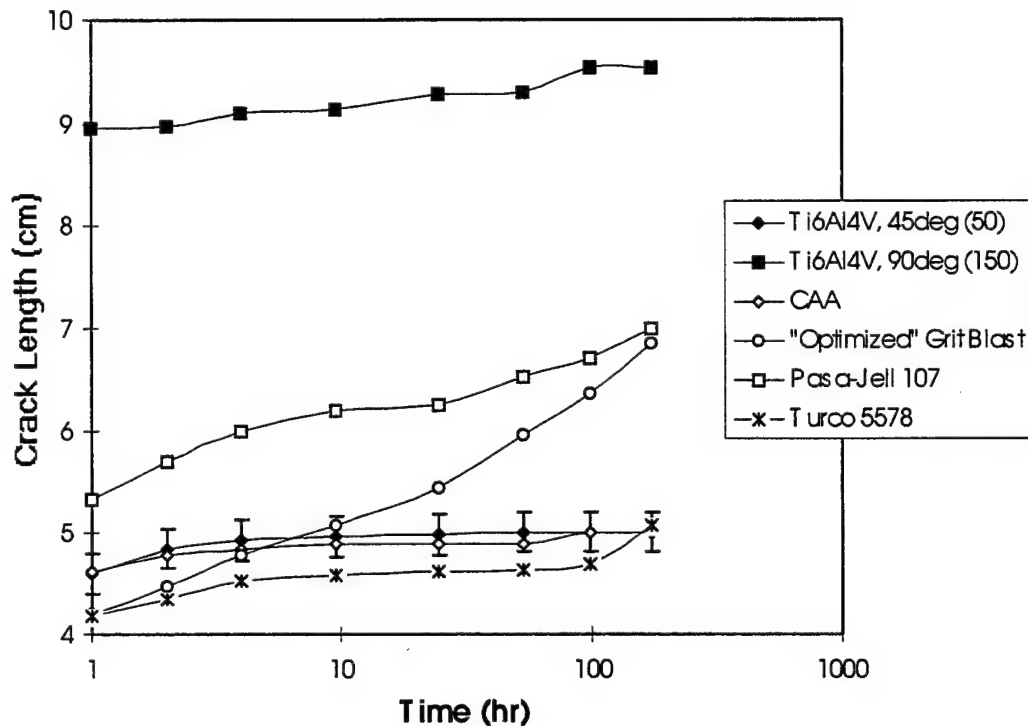


Figure 24. Wedge test performance of titanium treatments using Cytec FM-300M.

The results also show the need for relatively thin coatings; the 150- $\mu$ m, 90° specimen gave poor performance with failure within the coating. From these data, we cannot separate the effects of the spray angle and the coating thickness; however, previous work, which was performed with a 90° angle with a nominal thickness of 50  $\mu$ m, showed excellent wedge test performance.<sup>1</sup> Such findings are consistent with the aluminum results – coating thickness is more important than spray angle in determining bond performance.

*Table 3. Loci of Failure for Initial Titanium Wedge Tests*

<i>Treatment</i>	<i>Dry</i>	<i>Wet</i>
Ti6Al4V, 50 $\mu$ m (2.0mil) , 45°	within adhesive	within adhesive
Ti6Al4V, 150 $\mu$ m (5.8mil), 90°	within coating	within coating
CAA	within adhesive	within adhesive
Turco 5578	within adhesive	adhesive/substrate
Pasa-Jell 107	within adhesive and adhesive/substrate	adhesive/substrate
"Optimized" Grit Blast	within adhesive	adhesive/substrate

Results from subsequent wedge tests are shown in Figure 25 for FM-300M and Figure 26 for FM-73. The specimens bonded with FM-300M were prepared by the second plasma sprayer and are similar to, but not as good as, the initial results. The locus of failure was initially in the adhesive even after humidity exposure began, but shifted to the adhesive-coating interface before the test was completed. We speculate that the morphology of the coatings is almost adequate for sufficient physical bonding with this adhesive, but that when the adhesive plasticizes in the presence of moisture it can disengage from the coating. The 1-mil coating gave the best performance, although the 0.5- and 2-mil coatings had final crack lengths within 5 mm of the 1-mil coating.

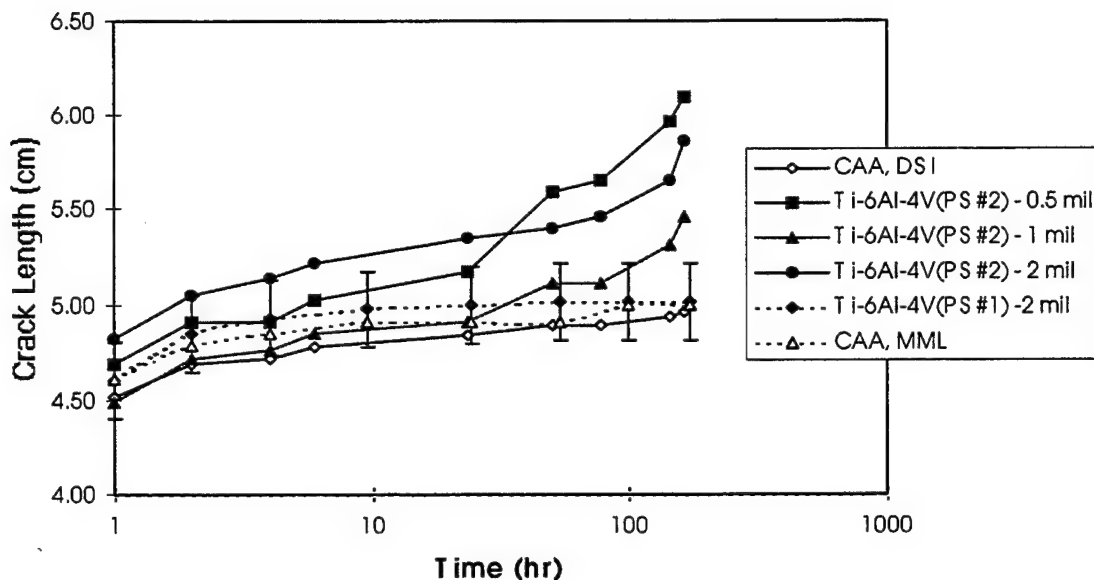


Figure 25. Subsequent wedge test involving plasma sprayed Ti-6Al-4V coatings on Ti-6Al-4V adherends. The adhesive was Cytec FM-300M. Also shown are some of the results from Figure 24. Please note the expanded scale of the figure.

The performance using FM-73 is not as good. With the exception of the coatings sprayed with the 150 mesh powder, all specimens failed within the adhesive under dry conditions despite the stronger adhesive. However, during moisture exposure, the crack propagation shifted to the interface. For this adhesive, the plasma sprayed Ti-6Al-4V on Ti-6Al-4V matched the Turco 5578 control treatment, but not the CAA. No significant difference was seen between specimens sprayed as 6x6" panels, bonded, then cut and specimens sprayed as 1x6" strips then bonded. The 0.5-mil coatings showed slightly worse performance than the 1.0- and 2.0-mil coatings. Confirming the data of Figure 24 no difference between the two sprayers. These specimens were sprayed using the same lot of powder used in Figure 15 (Al) and Figure 24 (Ti). Both sprayers used nominally identical powder, but different lots.

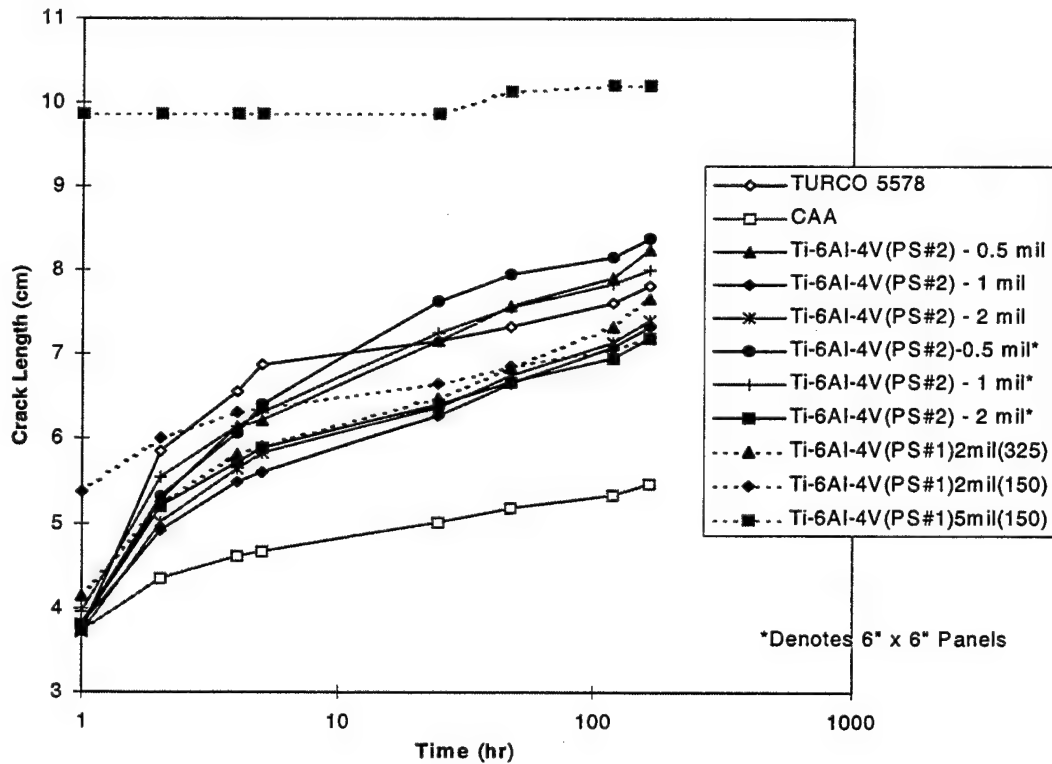


Figure 26. Wedge test results showing plasma sprayed Ti-6Al-4V coatings on Ti-6Al-4V adherends. The adhesive was Cytec FM-73M. The numbers in paratheses indicate powder size.

Not shown in Figure 26 are results of INCONEL sprayed coatings. The 5-mil INCONEL coating gave very poor performance with dry coating failure and interfacial moist failure. There were signs of corrosion.

One final wedge test was performed to test different Ti-6Al-4V spray conditions. The results, shown in Figure 27, were slightly better than those of Figure 26, but not close to that of CAA. The gun-to-specimen distance had little effect in going from 10 cm or 4 in. (the standard distance) to 7.5 cm or 3 in. The two powder sizes used (325 mesh and a blend of 75% 325 mesh and 25% 150 mesh) gave similar results. Crack propagation under dry conditions was mostly cohesive in the adhesive although there were areas on

some specimens, primarily along the edges, that were in the coating. The similarity in the initial crack length for all specimens suggests that the cohesive strengths of the coating and the adhesive are nearly the same. Under moist conditions, the locus of failure shifts to the interface for all specimens except CAA which remained mostly cohesive with some areas of interfacial failure.

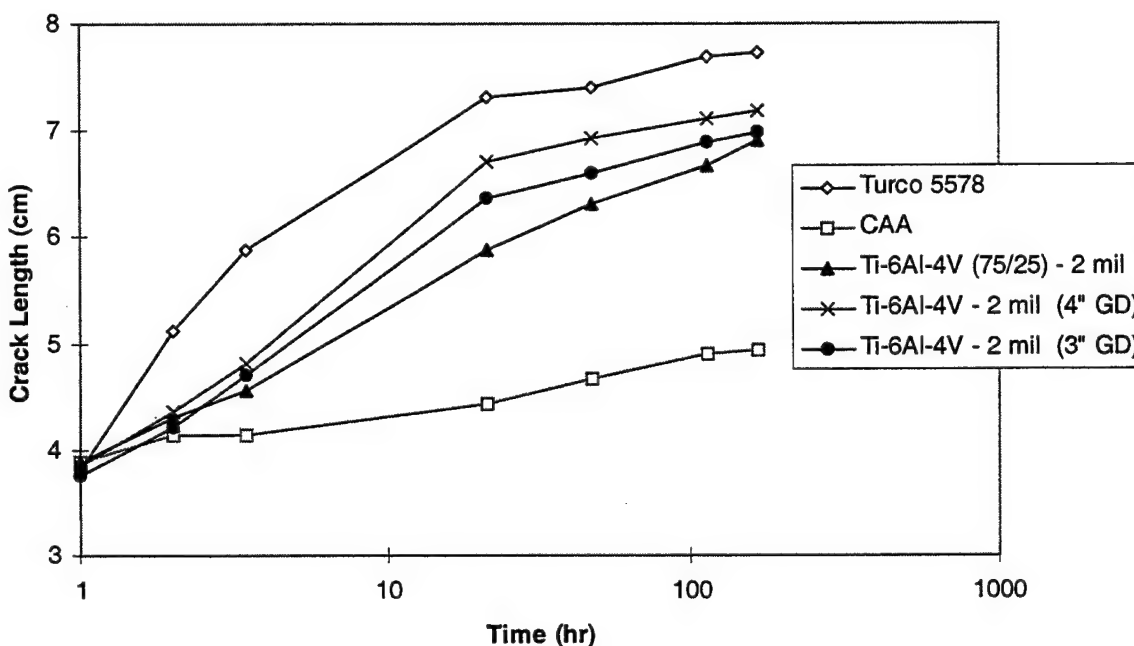


Figure 27. Wedge test results showing plasma sprayed Ti-6Al-4V coatings on Ti-6Al-4V adherends. The adhesive was Cytec FM-73M. The (75/25) denotes a mixture of 75% 325 mesh and 25% 150 mesh powder; gun distance was 4". The (4" GD) and (3" GD) denote the gun-to-surface distance; powder was 325 mesh. The specimens were prepared by PS#1.

The effect of priming was also evaluated for these specimens. The results are given in Figure 28. Priming clearly improves wedge test performance. Because of the stability of the titanium surface, the improvement is likely due to improved wetting rather than

the improved corrosion/hydration resistance. The two outside primed specimens exhibited much longer initial (and final) crack lengths than the two inside specimens. The outside specimens had some areas of apparent coatings failure under dry conditions. We speculate that the poorer performance was caused by either edge effects during plasma spraying or primer that was too thick. Occasional outliers have been observed when one or two specimens behave differently (worse) than the others cut from the 15x15-cm (6x6-in.) bondment. Most often, these have been at or near an edge of the 15x15-cm bondment. Such differences might be attributed to raster patterns, making the edge thicker, or temperature differences. Alternatively, because the primer was applied by brush, it was too thick and could have weakened the bond. Both the average over all four specimens and the average of the best performing specimens are given in Figure 28. The good specimens perform nearly as well as the CAA specimens; they are within the envelop of CAA performance as shown in Figure 29. It is expected that proper priming procedures (spraying) would allow the plasma-sprayed specimens to equal the CAA performance. The results suggest that, with FM-73, priming of the plasma-sprayed surfaces is required for best performance. For FM-300M, priming was not needed.

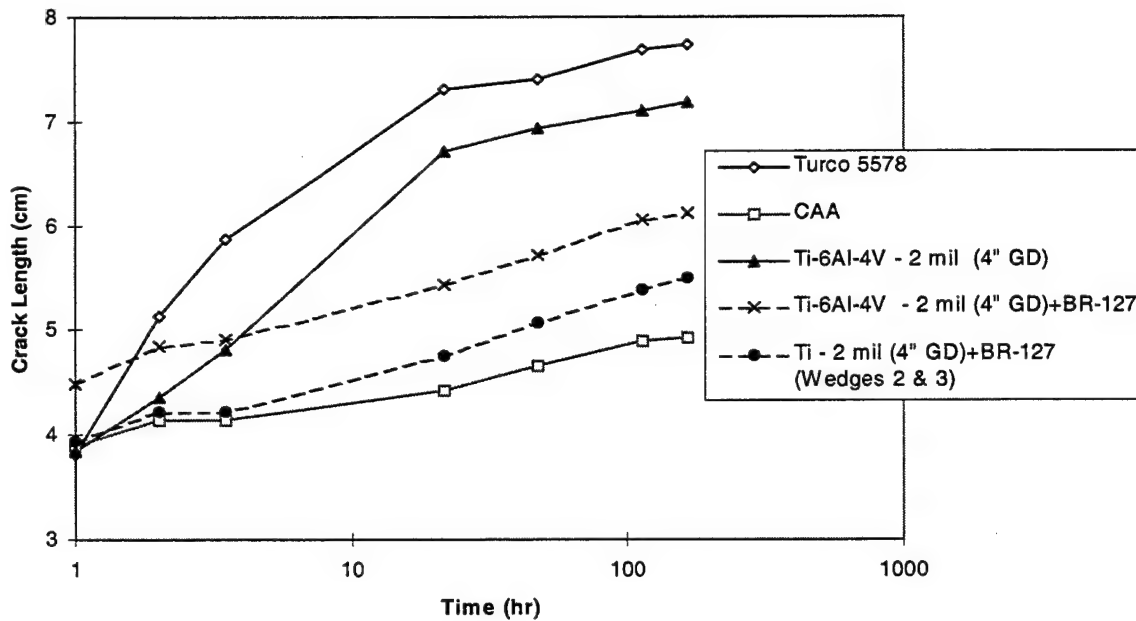


Figure 28. Wedge test results showing plasma sprayed Ti-6Al-4V coatings on Ti-6Al-4V adherends. The adhesive was Cytec FM-73M. Cytec BR-127 primer was used on one set of specimens. The specimens were prepared by PS#1.

The difference in performance for the two adhesives is not limited to the plasma-sprayed treatments. The CAA process gives consistent performance from time to time (Figure 29). The final crack length is independent of these two adhesives despite the increased initial crack length of the FM-300M adhesive. The Turco 5578 performance is very different for the two adhesives. With FM-300M, it performs as well as CAA, but with FM-73, it exhibits poor performance. For both adhesives, the crack propagates interfacially under moist conditions. Because of the stability of the titanium surface, we attribute these differences to morphology differences. The Turco and plasma spray surfaces are rough on a larger scale than the CAA surface and do not provide a density of physical bonding as high as the CAA surface.<sup>17,22</sup> Because the FM-73 adhesive absorbs more moisture than the FM-300M adhesive, it is better able to disengage from

the coarser adherend, especially if wetting is not complete. In comparison, the CAA surface generates very strong capillary forces to aid in the wetting process and forms a very high density of physical bonds to mechanically interlock with the adhesive even after moisture absorption. Thus priming may be necessary for plasma sprayed titanium adherends when FM-73 is used. Similar arguments may apply to aluminum as well, although, in some cases, unprimed plasma-sprayed adherends can match PAA performance.

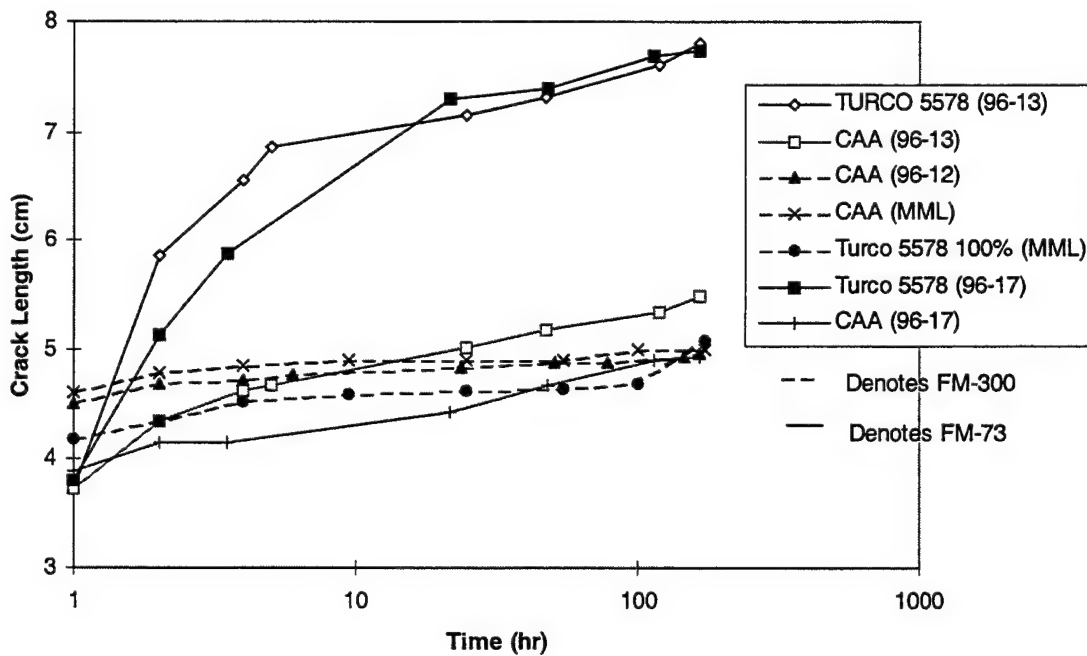


Figure 29. Wedge test results for titanium chemical control treatments for both Cytec FM-73 and FM-300M.

## 4. Electrochemical Studies

### 4.1 Hydration as a Bond Failure Mechanism

Electrochemical Impedance Spectroscopy (EIS) measurements were taken on an FPL-etched aluminum specimen with cured Cytec FM-123 adhesive (an adhesive half joint). Bode magnitude and phase angle representations are given in Figure 30 and Figure 31 for representative exposure times. Several changes are noted including a more than 100-fold decrease in the near dc resistance ( $\nu < 1000\text{Hz}$ ) and a more than 100-fold increase in the breakpoint frequency ( $\alpha = 45^\circ$ ), where the coating behavior changes from being mostly resistive (independent of frequency) to mostly capacitive (slope of -1 on log impedance vs log frequency plots). These two parameters are shown as a function of exposure time in Figure 32 and Figure 33. The two parameters exhibit trends that are the mirror image of each other. The graphs show four stages:

1. 0-10 days      Very rapid change
2. 10-100 days    Stabilization and little change
3. 100-150 days    Rapid change
4. 150-190 days   Stabilization and little change.

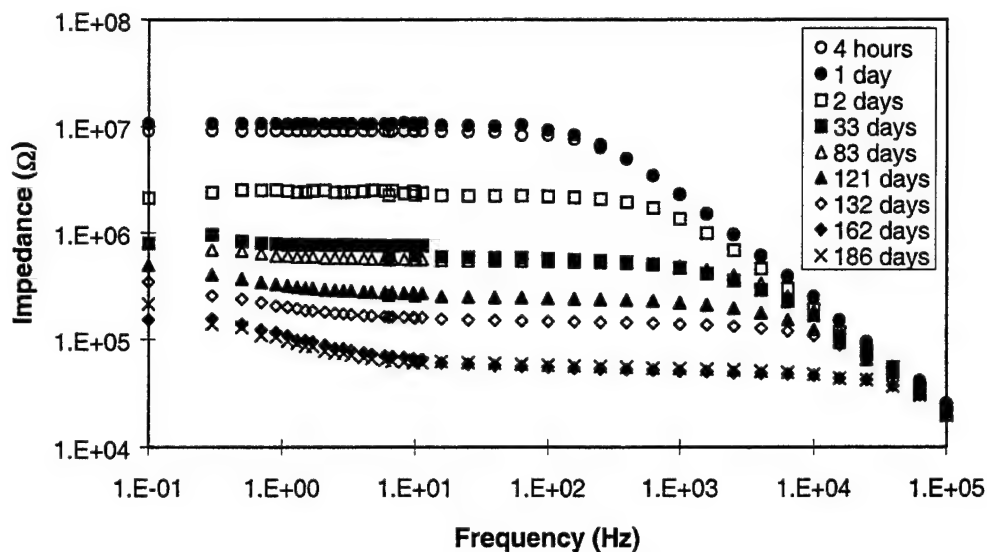


Figure 30. Bode representation of EIS data -- impedance magnitude versus frequency -  
- for open-faced aluminum bond immersed in hot water. Only representative times are  
shown for clarity.

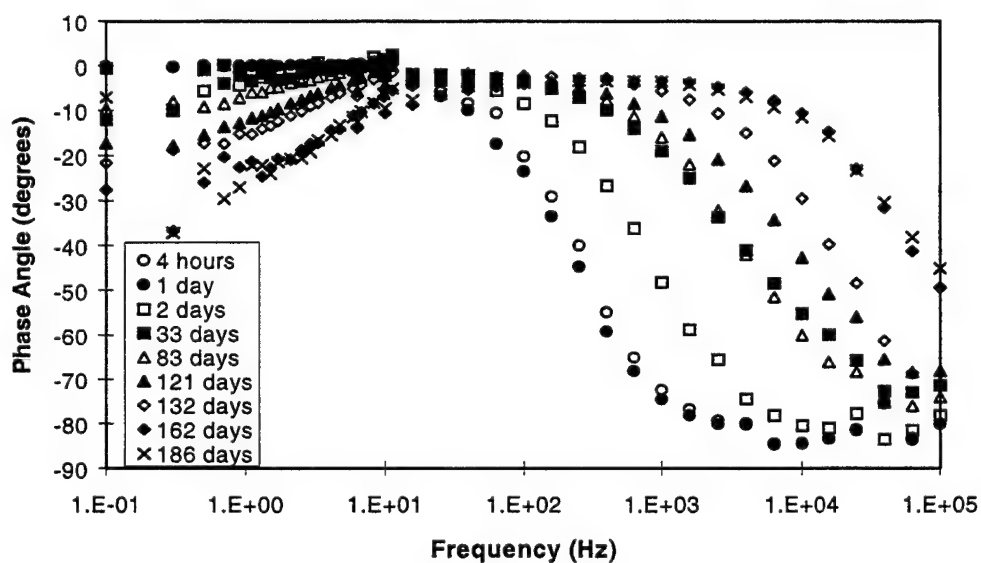


Figure 31. Bode representation of EIS data -- phase angle versus frequency -- for  
open-faced aluminum bond immersed in hot water.

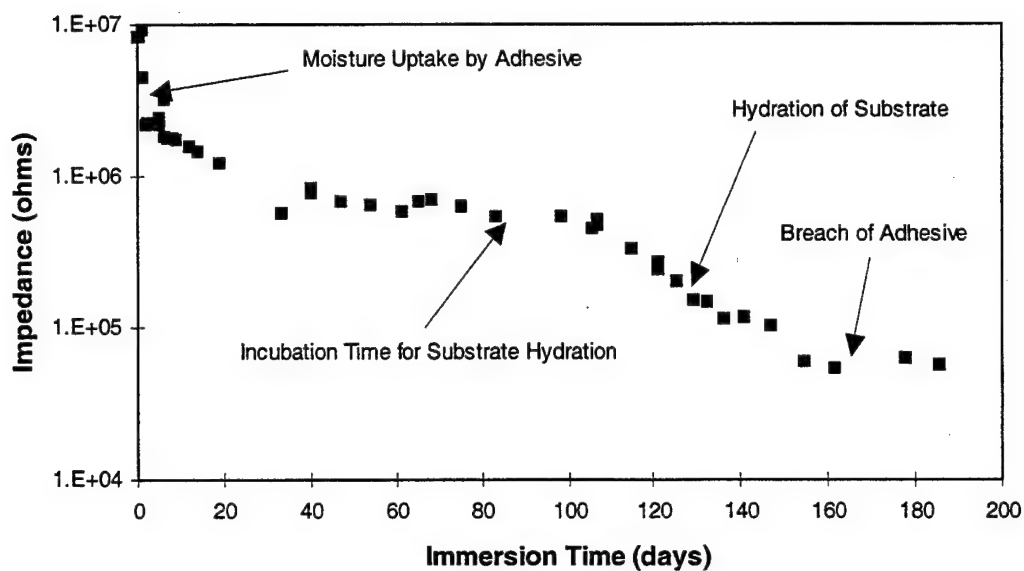


Figure 32. Near dc impedance (measured at 100 Hz) for the open-faced aluminum bond as a function of immersion time. The data can be divided into four stages as discussed in the text.

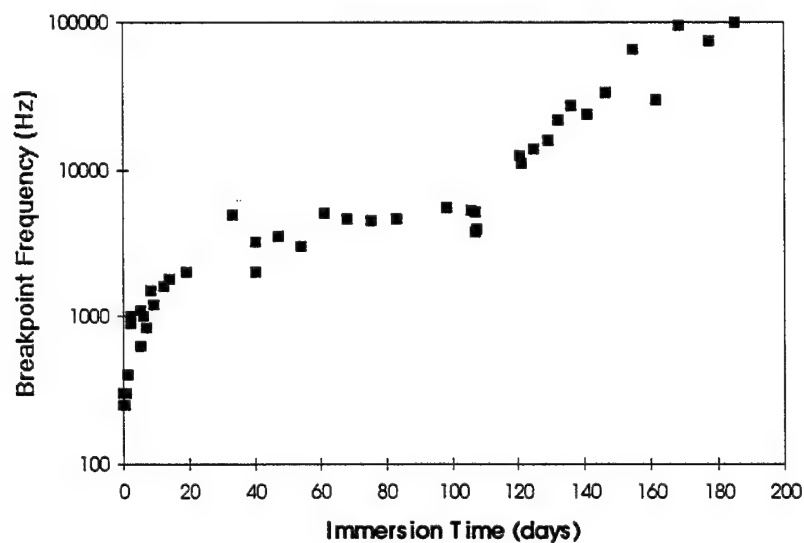


Figure 33. Breakpoint frequency for the open-faced aluminum bond as a function of immersion time. The data can be divided into four stages as discussed in the text.

It should be noted that a small fraction of the decrease in impedance in Stage 1 can be attributed to the temperature change. In raising the temperature to 58°C, the conductivity of the adhesive increased (resistivity or impedance decreased) by approximately a factor of two. Allowing the temperature to return to ambient increased the impedance to its value prior to heating the water bath. Despite this change in experimental conditions, most of the change indicated in the figures represents changes of the specimen with exposure time. No significant change in the breakpoint frequency was noted with temperature; consequently all of the increase observed in Figure 33 reflects actual changes in the specimen.

Visual inspections showed little change in the specimen, except for a fading of the color of the adhesive, until Stage 3. At that point, an anomalous area was observed at the edge of the exposed region. After removing the specimen from the fixture, this region resembled white "mountains" in a sea of adhesive. XPS analysis showed this material to be hydrated alumina erupting through the adhesive.

Results for the second "half-joint" specimens are given in Figure 34. These specimens included FPL, PAA, and P2 treatments with both FM-123 and FM-300M. Unfortunately, the humidity chamber malfunctioned with the temperature rising uncontrollably and destroyed the specimens so that longer exposure to hot water was not possible. The data to that point clearly show differences in the rate of water absorption (Phase 1 of Figure 32) with the FM-123 absorbing more water and the specimens reaching Phase 2 while FM-300M absorbed less water and the specimens remaining in Phase 1. During the period of the measurements, no difference was seen between the three surface prepa-

rations. Had the experiment continued, we would expect the FPL specimens to begin to hydrate first, followed by P2 specimens, and then PAA specimens.

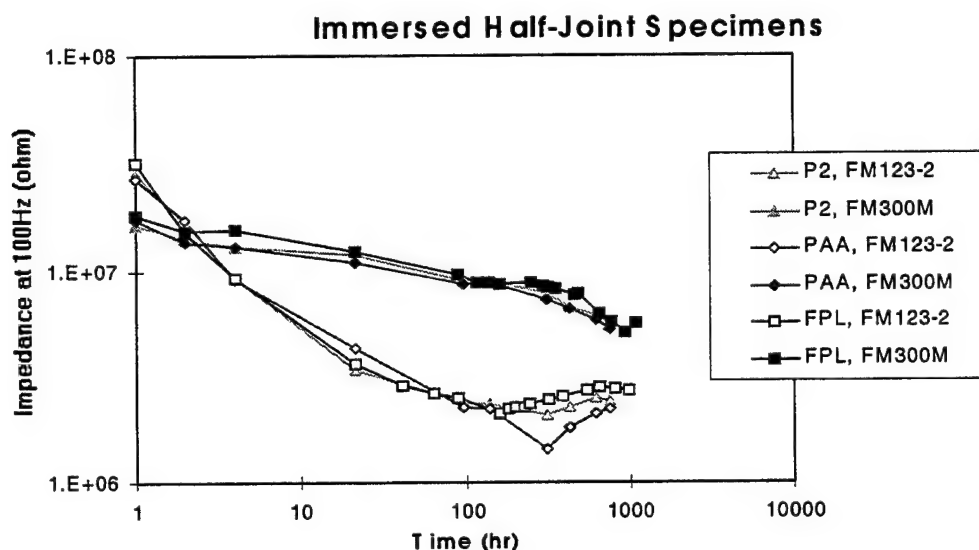


Figure 34. Near dc impedance as a function of time for aluminum specimens immersed in 75°C water.

The electrochemical measurements and the long-term immersion of the open-face aluminum bond provide two very important findings: 1) hydration of an aluminum surface occurs under an adhesive and 2) EIS measurements can detect this hydration.

Many investigators,<sup>14-19,23-25</sup> have concluded that, in a moist environment, an aluminum oxide surface will hydrate first to boehmite and then to bayerite. If this occurs under an adhesive, the resulting increase in volume will induce high stresses at the bondline and the poor adhesion of the hydroxide to the metal will allow crack propagation to relieve this stress. The evidence for this hydration-induced failure mechanism came from analysis of bare surfaces following exposure to moisture and of wedge test specimens in regions near the crack tip where the crack had propagated. Others<sup>26-28</sup> have ques-

tioned whether hydration occurs at an intact polymer-metal interface or only at metal (oxide) surfaces exposed directly to moisture. In the case of wedge test specimens, the hydration would occur after the crack had propagated past that point. Because the two arguments were circular -- the crack will not propagate interfacially until hydration occurs and hydration will not occur until the crack propagates interfacially -- experiments to date were not conclusive.

The current experiment is conclusive, however. The specimen had no crack and the edges were sealed from moisture. The only way moisture could reach the substrate surface was to migrate through the adhesive. Not only did the substrate hydrate, but the hydration products erupted through the adhesive. If the specimen had been an aluminum-aluminum joint, the local strength of the bond would have been reduced to zero and the growth of hydration products would generate stresses that would result in crack growth. Thus, one mechanism by which crack propagation in a moist environment is induced is hydration of the aluminum substrate.

It is also interesting to note the relative time scales of the different laboratory experiments and those of practical applications. In the open-faced adhesive joint experiment, the moisture had free access to the face of the adhesive, but not to the edges. Migration was through the thickness of the adhesive. Despite using a water-wicking adhesive without a corrosion-preventative primer and a surface preparation that is prone to hydration, approximately 4 months at 58°C was needed for the onset of hydration (Stage 3). By comparison, a wedge test, in which moisture has access to the crack tip and the joint is under opening stress, interfacial crack growth is observed within hours of humidity exposure and the test is commonly completed within 7 to 10 days. In the other ex-

treme, a practical bonded joint would commonly involve a hydration-resistant surface and a corrosion-resistant primer and would be exposed to moisture and high temperatures only sporadically. Furthermore, until a crack opens, moisture would need to diffuse in from edges that should be sealed according to best practices.

The detection of hydration by EIS was straightforward (at least, detection that changes were occurring was straightforward; associating those changes with hydration required post-test analysis). We can associate the four stages of the EIS measurements with the following events:

1. Absorption of moisture into the adhesive. A liquid double layer may form at the adhesive-oxide interface.
2. Incubation time for hydration.
3. Hydration.
4. Direct contact of the moisture with the hydration products/metal.

In Stage 1, water reaching the interface will preferentially bond to the oxide, thus breaking the weak secondary bonds that provide the chemical component of the interfacial bond.<sup>19,26</sup> If there are no physical bonds across the interface, i.e., there is no mechanical interlocking, interfacial strength will be lost and delamination will occur. This is the case with most protective coatings on grit-blasted or cleaned substrates. Consequently, this stage has been the most investigated with EIS.<sup>6-13</sup> For example, in the study correlating tensile strength with near-dc impedance, the impedance fell steadily and, after only 5 days of exposure to 1-ppm SO<sub>2</sub> and moisture, only 30% of the interfacial strength remained.<sup>11-13</sup> Up to a certain point, if corrosion of the substrate is mini-

mal, much of the loss of adhesion can be reversed if the system is dried so that the secondary bonds can reform. In a properly prepared aluminum bonded structure using FPL-, PAA-, or CAA-treated adherends, the microscopically rough aluminum oxide remains intact and maintains the physical bonding that provides interfacial strength even in the presence of moisture.

Stage 2 corresponds to the incubation time for hydration of the aluminum substrate.

This incubation time depends on the stability of the surface, the amount of water present at the interface, temperature, pH of the water, and other factors. It can be as low as 2 minutes for FPL surfaces immersed in 80°C water;<sup>17</sup> in this experiment, it was approximately 100 days. Interfacial strength is maintained during this period.

Hydration occurs during Stage 3. The second decrease in impedance and increase in breakpoint frequency is caused by the growth of the hydration product and breaching of the adhesive film allowing moisture freer access to the metal substrate. In our case, growth of the hydration “mountains” may have also broken the seal around the specimen and allowed the electrolyte to reach the backside of the substrate. At this point, local adhesion is lost. If this had been a complete joint, the expansion of the oxide as it is hydrated would have induced local stresses and allowed an interfacial crack to initiate and propagate. Nonetheless, in our specimen local adhesion appears to be maintained away from the “mountains” where hydration has not yet occurred.

In the final stage, hydration is continuing, but further changes in the impedance and breakpoint frequency are small. These parameters are being controlled by the existing hydration products and breach of the adhesive.

## **4.2 EIS as a Bond Monitor**

EIS measurements performed on wedge test specimens using the adherends as electrodes show the low-frequency impedance to be very sensitive to the amount of moisture in the bondline. Two experiments were performed: one in which the measurements were taken while the specimens were inside the humidity chamber and one in which the measurements were taken while the crack lengths were being marked outside the humidity chamber.

The near-dc impedance for the specimens measured inside the humidity chamber is given in Figure 35 as a function of time and in Figure 36 as a function of crack length. There is a very rapid decrease in impedance in the first hour of humidity exposure as moisture is wicked into the crack-tip region and the adhesive. After this first hour, there is little additional decrease although FM-300M specimens take several hours to reach the lowest potential, reflecting the reduced permeability of FM-300M to moisture.

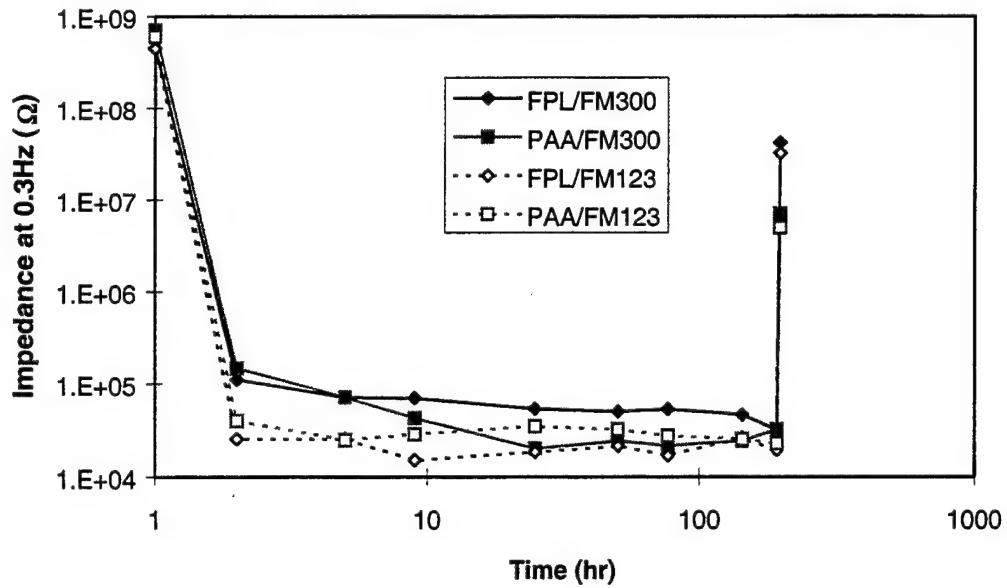


Figure 35. Near-dc impedance of wedge test specimens as a function of time. The EIS measurements were performed in the humidity chamber. The last data points were acquired at the end of the experiment after the specimens had dried.

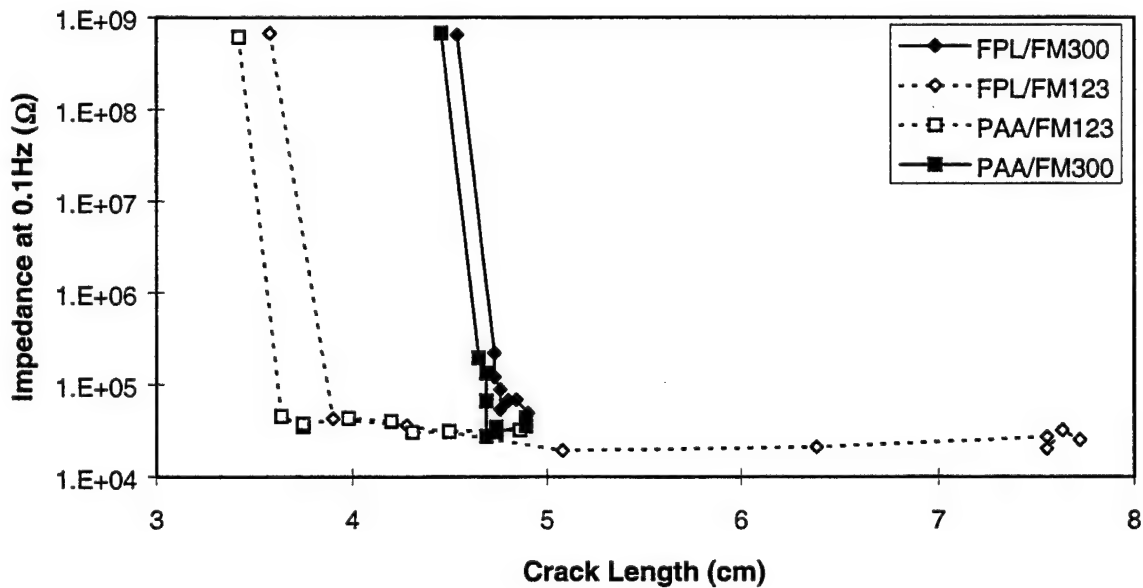


Figure 36. Near-dc impedance of wedge test specimens as a function of crack length. The EIS measurements were performed in the humidity chamber.

The data indicate that the EIS measurements are extremely sensitive to moisture intrusion into the bondline, but are not very sensitive to crack length, at least in this range (ultimately, if the bond completely separated, the impedance would become infinite). The very rapid decrease suggests that the presence of moisture at the crack tip, and not diffusion of moisture into the adhesive or along the interface, governs the impedance in this experiment. Nonetheless, because moisture is a root cause of bond degradation, this moisture sensitivity would serve as an early warning of the degradation process. Although measurements are dominated by the moisture intrusion, once the specimens are dried, there is a difference between the FPL and PAA measurements, both in the slope of the low-frequency region of the spectra and the magnitude of the near-dc impedance. The higher impedance of the FPL specimens likely reflects the greater hydration of these adherend surfaces. These data suggest that the impedance after drying is controlled by crack tip region and the hydration products of the FPL surface reduce the amount of current between the two adherends.

EIS measurements taken while the specimens were out of the humidity chamber show similar behavior (Figure 37 and Figure 38). The impedance again drops several orders of magnitude during initial exposure, but not as rapidly as the in situ measurements. The difference reflects the greater amount of moisture condensed in the crack tip region for the specimens with EIS measurements taken in the humidity chamber compared to those specimens whose measurements were taken out of the chamber while their crack tip region was partially drying. For consistency, the particular ex situ specimen shown in Figure 37 was always the first one to be marked for crack length and the EIS measurements taken. The impedance is governed by the profile (extent and con-

centration) of moisture in the adhesive as the moisture reduces the resistivity of the polymer. The increase in impedance after the first few hours may be related to the amount of moisture the FM-123 epoxy adhesive could uptake. At small crack lengths, there is considerable tensile stress at the crack tip and the adhesive can absorb more moisture than unstressed or less stressed adhesive (corresponding to longer crack length). Toward the end of the wedge test, EIS measurements were also taken on ex-situ specimen #1 (Figure 37) after all five specimens had been tested. The difference between the initial and subsequent measurements reflects the extent of moisture penetration – at longer exposure times, moisture has penetrated deeper into the adhesive (farther from the edge) and requires longer times to diffuse back out during drying. Hence, less change is observed during the short period out of the humidity chamber while crack lengths are marked and EIS measurements are obtained.

The EIS measurements of wedge test specimens demonstrate that this technique is very sensitive to the presence of moisture in the bondline. The near-dc impedance dropped more than three orders of magnitude with the presence of moisture at the crack tip. Although this configuration (crack under opening stress in a hot, humid environment) represents a worst case scenario, the extreme sensitivity suggests that the technique could detect much smaller amounts of moisture. Work performed on another program has demonstrated this use of EIS.

Importantly, the detection of moisture occurs before hydration or permanent degradation. For example, in the very accelerated conditions of Figure 32, moisture ingress into the adhesive was detected in the first day although hydration did not occur until more than 100 days afterward. Use of EIS to detect moisture gives warning before the joint

deteriorates and structural integrity is compromised. Appropriate maintenance, including heating to drive off the moisture or resealing the edges to prevent additional moisture ingress, could then be scheduled to prevent structural damage.

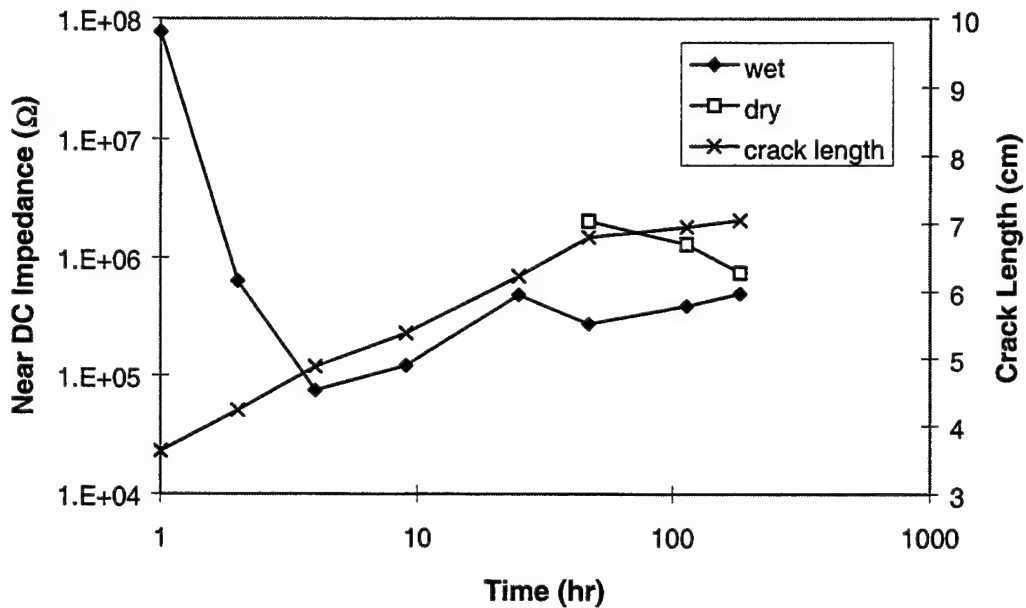


Figure 37. Magnitude of the impedance at 3.3 Hz as a function of time since crack initiation for the wedge test specimen. The "wet" data were taken immediately after removal from the humidity chamber; the "dry" data were taken after the other specimens were measured and the specimen had a chance to dry. Also shown is the propagated crack length.

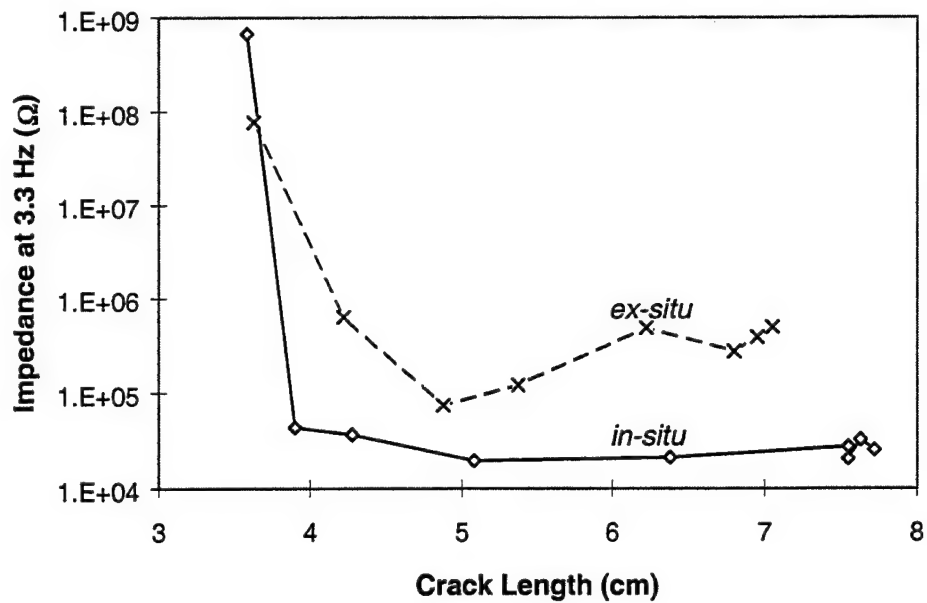


Figure 38. Near-dc impedance of wedge test specimens (FPL, FM-123) as a function of crack length. The in situ measurements were taken in the humidity chamber (Figure 35). The ex situ measurements were taken out of the humidity chamber (Figure 37).

## 5. Summary and Conclusions

This investigation has shown that plasma-sprayed coatings can provide very good to excellent bond performance (minimal initial crack length and crack growth during wedge testing) for aluminum and titanium adherends. In some cases, failure occurs within the adhesive -- the ultimate performance standard of a surface preparation. However, there are variability and reproducibility issues that need to be resolved before these coatings are used in high performance applications. Specific conclusions include:

### Aluminum Adherends

- Plasma-sprayed coatings are microscopically rough with irregular features of the order of micrometers that provide opportunities for physical bonding or mechanical interlocking with an adhesive or primer. The presence of smaller features ( $<1\mu\text{m}$ ) that provide a greater density of physical bonds is dependent on the initial powder and spray conditions. For aluminum/polyester composite coatings, migration of the adhesive can be detected through the coating.
- Initial bond strengths equal to that of the chemical controls with failure within the adhesive were obtainable for all-metal coatings (e.g., Ti-6Al-4V) and some alumina for all adhesives tested. Initial wedge test crack lengths were more sensitive to initial strength than tensile button pull measurements because of the weaker room-temperature curing epoxy. Early tests demonstrated the need for grit blasting or other pretreatment of the substrate prior to spraying to ensure good adhesion to the base metal.

- The best performing plasma spray treatments for aluminum were Ti-6Al-4V coatings. They could provide crack propagation wedge test performance equal to that of PAA for FM-73. In one case, the initial crack was so short that the aluminum adherends were permanently bent. However, there was considerable variation in performance with raw material (powder) or other variables. Better control of process variables will need to be established before application of this process. Use of a primer appears to be beneficial with FM-73 adhesive; a primer does not appear as necessary with FM-300M adhesive.
- Blends of aluminum and either polyester or PEEK provide good to excellent wedge test performance in terms of crack growth. The best performing treatments (aluminum/polymer blends with 20-40% polymer) provide wedge test performance equivalent to PAA for FM-300M adhesive and intermediate to FPL and PAA for FM-123 and FM-73 adhesives. Crack propagation is predominately through the polyester phase.
- The aluminum and polymer act synergistically to provide better results than either component individually -- the aluminum provides the structural framework of the coating and adhesion to the substrate; the polymer toughens the coating and may add supplemental chemical bonding to the physical bonding provided by the microscopically rough surface. Mixing of the powder during spraying operations is important. Electrostatic charging and clumping of powder grains can make the coating more heterogeneous than desired and lead to reduced performance.
- Thickness of the coating can be important. Coatings of approximately 12-50  $\mu\text{m}$  (0.5 - 2 mils) provide better performance than those of 150  $\mu\text{m}$  (6 mils).

- The performance of grit-blasted substrates is highly dependent on blasting parameters. Wedge test performance can range from very poor with the crack rapidly propagating to the end of the specimen to good with performance better than FPL for FM-123 adhesive.
- Comparison of results with FM-123 and FM-300M adhesives can give insight into failure mechanisms. Treatments for which the limiting factor in crack propagation is the rate of moisture ingress will exhibit significant reduction of final crack length with FM-300M adhesive compared to FM-123. Others will show less difference.
- Plasma spray treatments appear to allow extended hold times between spraying and bonding without degradation of bond strength. No primer is needed during this extended hold time.

#### **Titanium Adherends**

- Ti-6Al-4V coatings on Ti-6Al-4V can provide excellent wedge test performance with failure entirely within the FM-300M adhesive. Initial and final crack lengths during the wedge test were identical to CAA and Turco 5578 treatments.
- Similar coatings appear to require a primer when FM-73M adhesive is used. The primer assures good wetting and maximized physical bonding. A similar behavior is observed for the Turco 5578 treatment. Even with the primer, failure appears to be interfacial by the end of the humidity exposure.

#### **Electrochemical Studies**

- Hydration of aluminum oxide is shown to occur under an adhesive with no moisture access to the substrate except by migration through the adhesive. This new evi-

dence proves that subadhesive hydration can occur. The resulting volume and morphology change leads to crack initiation and propagation interfacially or within the hydrated layer.

- EIS measurements of both near dc impedance and breakpoint frequency detected ingress of moisture to the interface and subsequent hydration of the oxide film.
- Use of adherends as electrodes allows EIS to be performed across a bondline (in the absence of rivets). Such measurements are very sensitive to moisture ingress. Thus, the EIS process shows promise as a means to detect bond deterioration before all strength is lost and delamination occurs.

## 6. References

- <sup>1</sup>H.M. Clearfield, G.O. Cote, K.A. Olver, D.K. Shaffer, and J.S. Ahearn, *J. Adhes.* **29**, 81 (1989).
- <sup>2</sup>R.A. Pike, V.M. Patarini, R. Zatorski, and F.P. Lamm, in *Proc. 6th Int. Symp. on Structural Adhesive Bonding*, (American Defense Preparation Agency, Washington, 1992).
- <sup>3</sup>K.L. Wolfe, S.R. Harp, J.W. Grant, and J.G. Dillard, "Plasma-Sprayed Aluminum and Titanium Adherends: II. Durability Studies for Wedge Specimens Bonded with Polyimide Adhesive," *J. Adhes.* (in press).
- <sup>4</sup>K.L. Wolfe and J.A. Dillard, "Plasma-Sprayed Aluminum and Titanium Adherends: III. Polymeric Coatings – The Durability Studies of Adhesively Bonded Aluminum and Titanium," *J. Adhes.* (in press).
- <sup>5</sup>G.D. Davis, G.B. Groff, L.L. Biegert, and H. Heaton, *J. Adhes.* **54**, 47 (1995).
- <sup>6</sup>K.M. Takahashi and T.M. Sullivan, *J. Appl. Phys.* **66**, 3192 (1989).
- <sup>7</sup>F. Mansfeld, *Corrosion* **37**, 301 (1981),
- <sup>8</sup>J.R. Scully, *J. Electrochem. Soc.* **136**, 979 (1989).
- <sup>9</sup>S.A. McCluney, S.N. Popova, B.N. Popov, R.E. White, and R.B. Griffin, *J. Electrochem. Soc.* **139**, 1556 (1992).
- <sup>10</sup>J.H. De Wit, *Progress in the Understanding and Prevention of Corrosion, Vol. 1*. (Institute of Materials, London, 1993), p. 240.
- <sup>11</sup>T.C. Simpson, P.J. Moran, W.C. Moshier, G.D. Davis, B.A. Shaw, C.A. Arah and K.L. Zankel, *J. Electrochem. Soc.* **136**, 2761 (1989).
- <sup>12</sup>T.C. Simpson, P.J. Moran, H. Hampel, G.D. Davis, B.A. Shaw, C.A. Arah, T.L. Fritz, and K.L. Zankel, *Corros.* **46**, 331 (1990).
- <sup>13</sup>T.C. Simpson, H. Hampel, G.D. Davis, C.O. Arah, T.L. Fritz, P.J. Moran, B.A. Shaw, and K.L. Zankel, *Prog. Organic Coatings* **20**, 199 (1992).
- <sup>14</sup>G.D. Davis, T.S. Sun, J.S. Ahearn, and J.D. Venables, *J. Mater. Sci.* **17**, 1807 (1982).
- <sup>15</sup>J.S. Ahearn, G.D. Davis, T.S. Sun, and J.D. Venables, in *Adhesion Aspects of Polymeric Coatings*, K.L. Mittal, ed., (Plenum Press, New York, 1983), p. 281.
- <sup>16</sup>G.D. Davis, *Surf. Interface Anal.* **9**, 421 (1986).
- <sup>17</sup>J.D. Venables, *J. Mater. Sci.* **19**, 2431 (1984).
- <sup>18</sup>J.D. Venables, D.K. McNamara, J.M. Chen, T.S. Sun, and R.L. Hopping, *Appl. Surface Sci.* **3**, 88 (1979).
- <sup>19</sup>G.D. Davis and D.K. Shaffer, "Durability of Adhesive Joints," *Handbook of Adhesive Technology*, K.L. Mittal and A. Pizzi, eds., (Marcel Dekker, New York, 1994), p. 113.

- <sup>20</sup> J.A. Marceau and E.W. Thrall, in *Adhesive Bonding of Aluminum*, E.W. Thrall and R.W. Shannon, eds., (Marcel Dekker, New York, 1985), p. 177.
- <sup>21</sup> M.H. Kuperman and R.E. Horton, in *Engineering Materials Handbook*, Vol. 3, *Adhesives and Sealants* H.F. Brinson, chm., (ASM International, Metal Park, Ohio, 1990), p. 801.
- <sup>22</sup> S.R. Brown, in *Proc. 27th Nat. SAMPE Symp*, (Society for the Advancement of Materials and Process Engineering, Azusa, CA, 1982), p. 363.
- <sup>23</sup> T.P. Hoar and N.J. Mott, *J. Phys. Chem. Solids* **9**, 97 (1959).
- <sup>24</sup> L. Kozma and I. Olefjord, *Mater. Sci. Technol.* **3**, 850 (1987).
- <sup>25</sup> D.M. Brewis, J. Comyn, and J.L. Tegg, *Int. J. Adhes. Adhes.* **1**, 35 (1980).
- <sup>26</sup> A.J. Kinloch, *Adhesion and Adhesives* (Chapman and Hall, London, 1987).
- <sup>27</sup> J.S. Compton, *J. Mater. Sci.* **24**, 1575 (1989).
- <sup>28</sup> W. Brockman, O.D. Hennemann, H. Kollek, and C. Matz, *Int. J. Adhes. Adhes.* **6**, 115 (1986).

## 7. List of Publications

1. G.D. Davis, P.L. Whisnant, D.K. Shaffer, G.B. Groff, and J.D. Venables, "Plasma Sprayed Coatings as Surface Treatments of Aluminum and Titanium Adherends," *J. Adhes. Sci. Technol.* **9**, 527 (1995).
2. G.D. Davis, P.L. Whisnant, and J.D. Venables, "Subadhesive Hydration of Aluminum Adherends and its Detection by Electrochemical Impedance Spectroscopy," *J. Adhes. Sci. Technol.* **9**, 433 (1995).
3. G.D. Davis, P.L. Whisnant, and J.D. Venables, "Detection of Subadhesive Hydration of Aluminum Adherends by Electrochemical Impedance Spectroscopy," in *Proc. 18th Annual Meeting Adhes. Soc.*, J.W. Holubka, ed., (Adhesion Society, Blacksburg, VA, 1995), p. 218.
4. G.D. Davis, P.L. Whisnant, G.B. Groff, D.K. Shaffer, and J.D. Venables, "Plasma Sprayed Coatings as Surface Treatments of Aluminum Adherends," *Proc. 41<sup>st</sup> Inter. SAMPE Symp.* (SAMPE, Covina, CA 1996) p. 291.
5. G.D. Davis, P.L. Whisnant, and J.P. Wolff, Jr., "Monitoring Adhesive Bond Integrity with Electrochemical Impedance Spectroscopy," *Proc. 41<sup>st</sup> Inter. SAMPE Symp.* (SAMPE, Covina, CA 1996), p. 544.
6. G.D. Davis, P.L. Whisnant, G.B. Groff, and J.D. Venables, "Use of Plasma Sprayed Coatings as Surface Treatments for Aluminum Adherends," in *Proc. 19<sup>th</sup> Annual Meeting Adhes. Soc.*, T.C. Ward, ed., (Adhesion Society, Blacksburg, VA, 1996), p. 268.

7. G.D. Davis, B.S. Wenner, G. B. Groff, and R.A. Zatorski, "Use of Plasma Sprayed Coatings as Surface Treatments for Aluminum Adherends," in *Proc. Annual Joint Service Pollution Prevention Conf.* (American Defense Preparedness Assoc., Arlington, VA, 1996), p. 376.
8. R.H. Turner, I. Segall, F.J. Boerio, and G.D. Davis, "Effect of Plasma Polymerized Primers on the Durability of Aluminum/Epoxy Adhesive Bonds," *J. Adhes.* **62**, 1 (1997).
9. G.D. Davis G.B. Groff, and R.A. Zatorski, "Plasma Sprayed Coatings as Treatments for Aluminum, Steel, and Titanium Adherends," *Surface Inter. Anal.* **25**, 366 (1997).

## 8. List of Presentations

1. "Plasma Sprayed Coatings as Surface Treatments of Aluminum Adherends," G.D. Davis, D.K. Shaffer, P.L. Whisnant, G.B. Groff, and J.D. Venables, 3rd Intl. Conf. on Adhesion and Surface Analysis (Loughborough, UK, April 1994).
2. "Plasma Sprayed Coatings as Surface Treatments of Aluminum and Titanium Adherends," G.D. Davis, D.K. Shaffer, P.L. Whisnant, G.B. Groff, and J.D. Venables, 41st Nat. Symp. Amer. Vacuum Soc. (Denver, CO, October 1994).
3. "Detection of Subadhesive Hydration of Aluminum Adherends by Electrochemical Impedance Spectroscopy," G.D. Davis, P.L. Whisnant, and J.D. Venables, 18<sup>th</sup> Annual Meeting Adhes. Soc., (Hilton Head Island, SC, February 1995),
4. "Use of Electrochemical Impedance Spectroscopy to Monitor Adhesive Bond Integrity, G.D. Davis, P.L. Whisnant, and J.D. Venables, 42<sup>nd</sup> Nat. Symp. Amer. Vacuum Soc. (Minneapolis, MN, October 1995).
5. "Use of Plasma Sprayed Coatings as Surface Treatments for Aluminum Adherends," G.D. Davis, B.S. Wenner, P.L. Whisnant, G.B. Groff, and J.D. Venables, 19<sup>th</sup> Annual Meeting Adhes. Soc., (Myrtle Beach, SC, February 1996).
6. "Use of Plasma Sprayed Coatings as Surface Treatments of Aluminum and Titanium Adherends," G.D. Davis, B.S. Wenner, P.L. Whisnant, G.B. Groff, and J.D. Venables, 41<sup>st</sup> Inter. SAMPE Symp. (Anaheim, CA, March 1996).
7. "Monitoring Adhesive Bond and Coating Integrity with Electrochemical Impedance Spectroscopy," G.D. Davis, C.M. Dacres, B.C. Taggart, B.S. Wenner, and P.L. Whisnant, 41<sup>st</sup> Inter. SAMPE Symp. (Anaheim, CA, March 1996).

8. "Monitoring Adhesive Bond and Coating Integrity with Electrochemical Impedance Spectroscopy," G.D. Davis, C.M. Dacres, B.C. Taggart, B.S. Wenner, and P.L. Whisnant, 4<sup>th</sup> Inter. Conf. Adhes. Surf. Anal. (Loughborough, UK, April 1996).
9. "X-ray Photoelectron Spectroscopy, Auger Electron Spectroscopy, and Secondary Ion Mass Spectrometry," G.D. Davis, ASM Inter. Educational Symp. (Oak Ridge, TN, April 1996) (INVITED).
10. "Plasma Sprayed Treatments for Aluminum and Titanium Adherends," G.D. Davis, B.S. Wenner, G.B. Groff, and R. Zatorski, AeroMat'96: 7<sup>th</sup> Annual Advanced Aerospace Materials and Processes Conf. & Exposition, (Dayton, OH, June 1996).
11. "Monitoring Coating and Bondline Integrity with an In-Situ Corrosion Sensor," G.D. Davis, Gordon Research Conference on the Science of Adhesion (Tilton, NH, August 1996) (INVITED).
12. "Use of Plasma Sprayed Coatings as Surface Treatments for Aluminum Adherends," G.D. Davis, B.S. Wenner, G. B. Groff, and R.A. Zatorski, Annual Joint Service Pollution Prevention Conf. (San Antonio, TX, August 1996).
13. "Plasma Sprayed Coatings as Treatments for Aluminum, Titanium, and Steel Adherends," G.D. Davis, 43<sup>rd</sup> Nat. Symp. Amer. Vacuum Soc. (Philadelphia, PA, October 1996). (INVITED).